

Determinants of mortality across a tropical lowland rainforest community

Nadja Rüger, Andreas Huth, Stephen P. Hubbell and Richard Condit

N. Rüger (nadja.rueger@uni-leipzig.de) and A. Huth, UFZ, Helmholtz Centre for Environmental Research – UFZ, Dept of Ecological Modelling, Permoserstr. 15, DE–04318 Leipzig, Germany. Present address for NR: AG Spezielle Botanik und Funktionelle Biodiversität, Univ. Leipzig, Johannisallee 21–23, DE–04103 Leipzig, Germany. – S. P. Hubbell, Dept Ecology and Evolutionary Biology, Univ. of California Los Angeles, Los Angeles, CA 90095, USA. – SPH and R. Condit, Center for Tropical Forest Science, Smithsonian Tropical Research Institute, Unit 0948, APO AA 34002–0948, USA. RC also at: National Center for Ecological Analysis and Synthesis, 735 State St., Santa Barbara, CA 93101, USA.

Tree mortality is an important process determining forest dynamics. However, in species-rich tropical forests it is largely unknown, how species differ in their response of mortality to resource availability and individual condition. We use a hierarchical Bayesian approach to quantify the impact of light availability, tree size and past growth on mortality of 284 woody species in a 50-ha long-term forest census plot in Barro Colorado Island, Panama. Light reaching each individual tree was estimated from yearly vertical censuses of vegetation density. Across the community, 78% of the species showed increasing mortality with increasing light. Considering species individually, just 29 species showed a significant response to light, all with increasing mortality at high light. Past growth had a significant impact on all but three species, with higher growth leading to lower mortality. For the majority of species, mortality decreased sharply with diameter in saplings, then levelled off or increased slightly towards the maximum diameter of the species. Diameter had the biggest impact on mortality, followed by past growth and finally light availability. Our results challenge many previous reports of higher mortality in shade, and we suggest that it is crucial to control for size effects when assessing the impact of environmental conditions on mortality.

Empirical knowledge on demographic rates across tropical tree species is required to predict likely changes of tropical forest dynamics under changing environmental conditions or disturbance regimes (Phillips et al. 2004, Purves and Pacala 2008). Tree mortality is an important component of demographic variation among tropical tree species. Species differ in their average mortality rates as well as in the response of mortality to resource availability (e.g. light, soil moisture) or individual condition (e.g. size, vigour) reflecting different life-history strategies. However, estimating mortality rates across diverse tropical tree communities is challenging because many species occur at low densities (Pitman et al. 1999, Condit et al. 2006, Chao et al. 2008) and assessing the effects of resource availability on mortality is even more demanding as it requires measurements of resource availability for many individuals (Lieberman et al. 1989).

Light is an important limiting resource in moist tropical forests (Poorter and Kitajima 2007) and horizontal and vertical light gradients represent a relevant source of environmental heterogeneity (Brokaw 1985, Denslow 1987). Research on the impact of light availability on mortality rates of tropical tree species has yielded inconclusive results. In a community-level study, no effect of light on mortality of seedlings was detected (Turner 1990). At the species level, several studies report mortality of seedlings to be lower

at higher light levels (Augspurger 1984, Kobe 1999, de Souza and Válio 2001, Montgomery and Chazdon 2002, Iriarte and Chazdon 2005, Aiba and Nakashizuka 2007, de Gouvenain et al. 2007). The only study also including adult trees, found lower mortality at higher crown exposure to light for four out of 11 *Macaranga* species in Borneo, while crown exposure did not have a significant effect on the remaining species (Davies 2001).

In contrast, Welden et al. (1991) found no statistical difference between sapling (1–4 cm diameter at breast height; dbh) mortality in gap versus non-gap sites for the majority (83%) of 148 woody species at Barro Colorado Island (BCI), Panama. Six and 19 species had significantly lower and higher mortality in gaps, respectively. However, when species were pooled into adult-stature categories (i.e. shrubs, understory treelets, midstory trees, canopy trees), mortality was consistently higher at high light. Likewise, mortality of tree, understory and liana seedlings was higher in large gaps compared to small gaps or closed forest (Dupuy and Chazdon 2006).

The importance of tree size for mortality is widely recognized (Turner 1990, Davies 2001, Aiba and Nakashizuka 2007, de Gouvenain et al. 2007). Therefore, it is crucial to control for tree size when environmental effects on mortality are evaluated. However, there are only few studies that simultaneously assess the light and size dependence of mortality at the species level for juvenile and adult life stages (Davies 2001, Metcalf et al. 2009).

Apart from light availability and tree size, tree vigour reflected by past growth may also be an informative predictor of mortality with slow-growing trees generally being at higher risk of mortality (Swaine et al. 1987, Kobe et al. 1995, Montgomery and Chazdon 2002, Chao et al. 2008, Wunder et al. 2008).

Our aim is to disentangle the effects of light availability, individual tree size and past growth on mortality rates of 284 woody species occurring at BCI. Forest census data from the 50-ha forest census plot at BCI provided information on the spatial location, size and fate of nearly 170 000 individuals in the census interval 1990–1995. Yearly canopy census data that recorded presence/absence of vegetation every 5 m in six height layers were used as a proxy for light availability for each individual tree. We used a hierarchical Bayesian approach to quantify the dependence of mortality on light, size and past growth across the entire tree community.

The hierarchical Bayesian approach combines probability models for the mortality between and within species with a model relating mean mortality rate to variation in light, tree size, and past growth (Clark 2005, Condit et al. 2006). Rare species are included in the analysis and contribute information, but correctly weighted by their abundance. The estimated parameters are directly relevant for understanding and forecasting forest change, and posterior probability distributions provide direct estimates of parameter uncertainty (Ellison 2004).

Methods

Study area

We analysed data from a 50-ha forest census plot on Barro Colorado Island (BCI), Panama ($9^{\circ}9'N$, $79^{\circ}51'W$). BCI is a 1567-ha island in the Panama Canal covered with tropical lowland moist forest. The plot consists of 48 ha of undisturbed old-growth forest and 2 ha of secondary forest about 100 years old (Foster and Brokaw 1982). The climate on BCI is warm throughout the year, but rainfall is seasonal with most of the 2500 mm falling during the wet season from April to November (Windsor et al. 1990). Elevation of the plot is 120–155 m a.s.l. (Hubbell and Foster 1983).

Mortality data

All free-standing woody individuals ≥ 1 cm dbh were mapped, identified to species and measured in 1981–1983, 1985, and every five years thereafter (< www.ctfs.si.edu>; Hubbell and Foster 1983, Condit 1998). Here we use the census interval from 1990–1995 and record the fate of each individual alive at the beginning of the census interval five years later. We included only individuals in the analysis that were alive also during the previous census interval from 1985–1990 and determined their past dbh growth (mm year^{-1}) during this interval. Growth rates ≤ 0 were arbitrarily set to 0.1 mm year^{-1} . To avoid edge effects of the light availability calculation, we excluded all individuals within 20 m of any edge of the plot. In total, 168 254 individuals of 284 species were included in the analysis.

Estimation of light availability

Yearly canopy censuses were conducted from 1983 to 1996, except for 1994. Thereafter, the canopy census was omitted for

several years and then continued applying a different canopy census method. Thus, consistent canopy census data are only available for the two census intervals 1985–1990 and 1990–1995, and we restricted our analysis to the second interval.

We use the canopy census data to produce an index of the amount of light reaching any point in the forest. The canopy census includes a record of the height at which vegetation intersected vertical lines above points on a square, 5-m grid across the 50 ha. Presence versus absence of vegetation was recorded in six height intervals, 0–2, 2–5, 5–10, 10–20, 20–30 and ≥ 30 m, with the assistance of an ocular range finder. A single census of all 20 301 points on the grid was done annually.

If vegetation was present in a height interval, we assume it casts shade below exactly as would a flat circle of diameter 5 m placed at the vertical midpoint of the cell (for the topmost height category, we assumed the circle was at 35 m height because few trees are taller than 40 m). For any point below, the vegetation obscures a section of the sky. Using trigonometry, we calculate the angle of sky so obscured by vegetation at position C, denoted α_c (Supplementary material Appendix 1). The total amount of sky obscured at any point P is the sum of α_c over all cells C that are near enough to cast shade; we assume that points with a horizontal distance of ≤ 20 m from C are near enough. These assumptions mean that each cell of vegetation reduces light, even if there is another cell above it: the top layer removes a certain quantity of light, and the next layer below removes more. This approach seems reasonable, in that several layers of leaves directly above a point reduce light to a level lower than a single layer would. The assumption that the presence of vegetation can be modelled as a horizontal circle of diameter 5 m is arbitrary.

We tested three alternative algorithms about how vegetation casts shade and all produced similar results. We acknowledge this is only a crude way of converting canopy density above a point to light reaching the point. However, by using many surrounding points and many vertical layers (cf. Connell et al. 1997), we suggest that this method may be somewhat better at estimating light than methods based only on taller trees within a 10 m radius (Lieberman et al. 1995) or the top layer of vegetation (Welden et al. 1991).

To convert the estimates of shading to an estimate of light availability, we calculated the mean shading index during 1990–1995 (no canopy census was done in 1994) for each point of the plot's 5-m grid at height $z = 2$ m, providing a probability distribution of the shade index.

Wirth et al. (2001) provide a probability distribution of irradiance I at one m height in December (i.e. the end of the rainy season) 1993 at BCI consisting of 396 direct measurements of relative irradiance. We matched their distribution of irradiance with our probability distribution of canopy shading, s . We assumed the 5th, 25th, 50th, 75th and 95th percentiles of the two distributions match, allowing a simple conversion of each value s to I by using the regression line through the percentiles (Supplementary material Appendix 1). Values of I range between 0.003 (deep shade) and 0.987 (full sunlight). A direct comparison between estimated light availability and light measurements is not possible because currently the canopy census is done in a different way, and there are no light measurements available for the years in which the canopy census was done as described here. However, the light index performed very well in predicting recruit numbers across 263 species at BCI (Rüger et al. 2009).

For the analysis, we calculated s at the top of each individual tree and converted it to relative irradiance as described. The height h of each tree was estimated from

$$h = h_{\max} (1 - e^{-a \times dbh^b})$$

where dbh is in cm and h_{\max} , a , and b were parameters fitted to data on measured height and dbh (Chave et al. 2003). The three parameters were fitted for all of the commoner species; for rare species, height was estimated using parameters of all height data pooled (see Table A1 in Chave et al. 2003 for parameters). Thus, for each individual tree we have an estimate of light at the top of its crown.

Variable selection

Because the hierarchical Bayesian model requires long computation times, we first performed independent logistic regressions of mortality as a function of light, dbh and growth to select the best explanatory variables. We first compared three variables describing tree growth using the Akaike information criterion (AIC; Akaike 1974): absolute growth rate, $\log(\text{absolute growth rate})$ and relative growth rate (growth/dbh). $\log(\text{growth})$ best predicted mortality for 73 out of 125 species with >100 individuals and was selected.

We then applied a step-wise procedure to determine the best predictors of mortality for the same 125 species and used AIC to compare models of different complexity. When dbh , $\log(dbh)$, light, $\log(\text{light})$ and $\log(\text{growth})$ were compared, $\log(\text{growth})$ was the best predictor for the largest number of species. Thus, we fixed $\log(\text{growth})$ as a first predictor and searched for the second best predictor. The second best predictor was $\log(dbh)$, significantly improving the prediction for 51 species ($|\Delta\text{AIC}| > 2$).

When dbh , light, $\log(\text{light})$ and an interaction between $\log(\text{growth})$ and $\log(dbh)$ were compared, dbh was the third best predictor, significantly further improving the prediction for 57 species. Likewise, when light, $\log(\text{light})$, and interactions between $\log(\text{growth})$ and $\log(dbh)$ or dbh were compared, $\log(\text{light})$ performed best, significantly improving the prediction for 33 species. Additionally, $\log(\text{light})$ was normally distributed, thus preventing distortion of mortality predictions for high-light conditions. Thus, $\log(\text{growth})$, $\log(dbh)$, dbh and $\log(\text{light})$ were included in the analysis as predictors of mortality. Including both $\log(dbh)$ and dbh allows for a U-shaped response of mortality to tree size (cf. Davies 2001, Metcalf et al. 2009).

Hierarchical Bayesian model

We used a hierarchical Bayesian framework (Clark 2005) to assess the light, size and growth dependence of mortality

across tree species at BCI. Data enter our model as the observation on a single individual i and whether it survived the census interval ($\text{alive}_i = 1$) or not ($\text{alive}_i = 0$). We assume that alive_i follows a binomial distribution with the predicted probability of survival p_i

$$\text{alive}_i \sim \text{binomial}(p_i)$$

Survival probability p_i of an individual is calculated from its predicted annual per capita mortality rate constant (m_i , % year $^{-1}$) and adjusted to the time period elapsed between its measurement in the first (t_1 , number of days since 1 January 1981) and second census (t_2)

$$p_i = e^{\frac{-m_i(t_2 - t_1)}{365.25}}$$

Mortality rate m_i is predicted from a logistic function including the dbh of individual i (dbh_i , mm), the light availability (l_i , unitless), and past growth (g_i , mm year $^{-1}$) as predictors and species-specific coefficients describing the mortality constant of a species j (a_j), the impact of light (b_j), size (c_j , d_j) and growth (e_j):

$$m_i = \frac{1}{1 + e^{-(a_j + b_j \times \log(l_i) + c_j \times \log(dbh_i) + d_j \times dbh_i + e_j \times \log(g_i))}}$$

To describe the variation of a , b , c , d and e across the community, we defined a hyperdistribution for each parameter. The specific type of distribution was chosen based on model runs without hyperdistributions (i.e. estimation of the posterior distributions for each species independently of the other species) which revealed that all model parameters were approximately normally distributed across the community. Thus, we used normal hyperdistributions for a , b , c , d and e , with hyperparameters μ_a , μ_b , μ_c , μ_d and μ_e describing the community-wide means and σ_a , σ_b , σ_c , σ_d and σ_e measuring the between-species variation. The runs without hyperdistributions also revealed that for species with >100 individuals, estimates of all parameters were largely determined by the data, whereas for species with <10 individuals, estimates were mostly determined by the community-wide mean.

As we did not have prior knowledge, we used non-informative flat priors for all parameters:

$$\mu_a, \mu_b, \mu_c, \mu_d, \mu_e \sim \text{uniform}(-10, 10)$$

$$\sigma_a, \sigma_b, \sigma_c, \sigma_d, \sigma_e \sim \text{uniform}(0, 2)$$

Altogether, the joint posterior distribution for the full model is

$$P(p, a, b, c, d, e, \mu_a, \sigma_a, \mu_b, \sigma_b, \mu_c, \sigma_c, \mu_d, \sigma_d, \mu_e, \sigma_e | \text{alive}, l, dbh, g)$$

$$\propto \prod_{j=1}^{\text{spp}} \prod_{i=1}^{n_j} \text{Binomial}(\text{alive}_{i,j} | p_{i,j}) \times \prod_{j=1}^{\text{spp}} \text{Normal}(a_j | \mu_a, \sigma_a) \times \prod_{j=1}^{\text{spp}} \text{Normal}(b_j | \mu_b, \sigma_b) \times \prod_{j=1}^{\text{spp}} \text{Normal}(c_j | \mu_c, \sigma_c) \times \prod_{j=1}^{\text{spp}} \text{Normal}(d_j | \mu_d, \sigma_d) \times \prod_{j=1}^{\text{spp}} \text{Normal}(e_j | \mu_e, \sigma_e) \times \text{Unif}(\mu_a | -10, 10) \times \text{Unif}(\mu_b | -10, 10) \times \text{Unif}(\mu_c | -10, 10) \times \text{Unif}(\mu_d | -10, 10) \times \text{Unif}(\mu_e | -10, 10) \times \text{Unif}(\sigma_a | 0, 2) \times \text{Unif}(\sigma_b | 0, 2) \times \text{Unif}(\sigma_c | 0, 2) \times \text{Unif}(\sigma_d | 0, 2) \times \text{Unif}(\sigma_e | 0, 2)$$

with spp being the number of species with living individuals at the beginning of the census interval and n_j the number of individuals of species j. The model assumes no correlation between parameters.

Model implementation and diagnostics

Posterior distributions of the species-specific parameters of the mortality model as well as the hyperparameters were obtained using a Markov chain Monte Carlo (MCMC) method that is a hybrid of the Metropolis–Hastings algorithm and the Gibbs sampler (Gelman et al. 1995, Condit et al. 2006). Parameter values are sequentially updated as in the Gibbs sampler, but acceptance depends on the likelihood ratios as in the Metropolis–Hastings algorithm. The proposal distribution is a normal distribution centred on the current value of the given parameter. The step width for each parameter, i.e. the standard deviation of the proposal distribution, is constantly adjusted during the burn-in period in such a way that acceptance rate is kept around 0.25 (Gelman et al. 1995).

To speed up the convergence of the Gibbs sampler, we weakened the correlation of a with b, c and d by centring the light and dbh data on rounded median or mean values across all individuals

$$m_i = \frac{1}{1 + e^{-(a_j + b_j \times (\log(l_i) - \log(\bar{l})) + c_j \times (\log(dbh_i) - \log(\bar{dbh})) + d_j \times (dbh_i - \bar{dbh}) + e_j \times \log(g_i))}}$$

with $\bar{l} = 0.05$ (median = 0.052) and $\bar{dbh} = 50$ mm (mean = 49.6 mm). Thus, $1/(1+e^{-a})$ represents predicted annual mortality of a tree with 5 cm dbh that receives 5% light and grew 1 mm year⁻¹ in the past census interval ($\log(1) = 0$). Coincidentally, mean growth of trees with dbh between 4 and 6 cm that receive between 4 and 6% light is 1.1 mm year⁻¹.

We monitored convergence by running two chains with different initial values and used the Gelman and Rubin's convergence diagnostics and a value of 1.1 to detect convergence (Gelman et al. 1995). Post hoc analyses showed that the correlation between model parameters was $\leq |0.25|$ for all parameter combinations. These correlations were not strong enough to prevent the chains from mixing well and convergence required 100 to 4600 iterations. We used a burn-in period of 15 000 iterations and additional 10 000 iterations were used for analysis. We computed posterior parameter distributions given observed survival, light availability, dbh and growth of each individual. All analyses were carried out using the software package R ver. 2.11.1 (R Development Core Team 2010) and simulations were run on parallel computers.

Analysis

From the posterior distributions we computed the mean and 95% credible intervals (CI) of all species-specific parameters of the mortality model and of the predicted annual mortality rate at 5 cm dbh, 5% light and 1 mm growth ($1/(1+e^{-a})$). Significance of coefficients was assessed by a CI that did not include zero. To evaluate

how uncertainty of parameter estimates decreased with sample size, we computed CIs for species with ~10, ~100, ~1000 and ~10 000 individuals. In 1990, there were 66 species with 1–10 individuals, 93 species with 11–100 individuals, 92 species with 101–1000 individuals, and 33 species with >1000 individuals. The fitted hyperdistributions have a larger variance than the species-specific means because they are fit to the distribution of the given model parameter across species at any step of the Metropolis–Hastings algorithm. In contrast, the species-specific means do not contain information on the variance of the posterior distribution and consequently their distribution has a lower variance.

To compare model predictions with data, we calculated observed mortality in different size classes. The number of size classes used depended on the abundance of the species. For species with ≤ 100 individuals, all individuals were pooled. For species with > 100 and ≤ 1000 individuals, observed mortality rates were computed for three dbh classes each containing a third of the individuals. For species with > 1000 individuals, observed mortality rates were computed for ten dbh classes each containing a tenth of the individuals. For species with > 2000 individuals, the largest dbh class was split further into different numbers of dbh classes each containing at least 100 individuals. We visualised the effect of light by drawing two curves of predicted mortality across the dbh range at 2% and 20% light, respectively, with growth fixed at mean growth of the species. Likewise, we draw two curves at slow growth (5th percentile) and fast growth (95th percentile), with light fixed at mean light experienced by individuals of the species.

We calculated contributions of light, dbh and growth to mortality by comparing mortality rates at standardised conditions. For saplings, we calculated the difference between predicted mortality at baseline conditions defined as 1 cm dbh, average light availability at 1 cm dbh (2%) and average growth at 1 cm dbh (0.35 mm year⁻¹) and mortality at higher light, larger dbh or faster growth. Mortality at higher light was calculated at average light + 1 SD (SD = 1.3% for individuals with dbh = 1 cm). The effect of larger size reflecting growth at a constant light level was assessed at 2.5 cm dbh, because still 6% of individuals with dbh between 2 and 3 cm occur at $\leq 2\%$ light. In this analysis only species with maximum dbh ≥ 2.5 cm were included. The impact of fast growth was evaluated for trees growing 1 SD faster than average (SD = 0.39 mm year⁻¹ for individuals with dbh = 1 cm).

For larger trees (only for species with maximum dbh ≥ 10 cm), we performed similar comparisons using mortality at 10 cm dbh, average light availability (18%) and average growth (2 mm year⁻¹) as a baseline. The impact of higher light was assessed at average light + 1 SD (SD = 11% for individuals with 9 cm $<$ dbh $<$ 11 cm). The effect of larger size was assessed at 25 cm dbh, because 8% of individuals with dbh between 24 and 26 cm occur at $\leq 18\%$ light. In this analysis only species with maximum dbh ≥ 25 cm were included. The impact of fast growth was evaluated for trees growing 1 SD faster than average (SD = 2.4 mm year⁻¹ for individuals with 9 cm $<$ dbh $<$ 11 cm).

Results

Community-level patterns of mortality

The hierarchical model produces a community-wide distribution of mortality parameters, based on results for all species and properly discounting rare species relative to common. This distribution should be taken as the best estimate of the community pattern, not the histogram of observed species' parameters, which is biased by rare species (Fig. 1).

Mean posterior estimates of the effect of log(light) on mortality (b) ranged from -0.15 to 0.63 , where negative means decreasing mortality at higher light (Fig. 1A; Supplementary material Appendix 2). For 269 species (95%) b was >0 , indicating increasing mortality at higher light levels. The 95% credible interval (CI) of b did not include zero in 29 species (10%). For these species mortality was significantly higher in higher light. These included shrubs (*Hybanthus prunifolius*, *Mouriri myrtilloides*, *Rinorea sylvatica*), under-story treelets (*Desmopsis panamensis*, *Swartzia simplex* var. *grandiflora*), midstory trees (*Garcinia intermedia*, *Protium panamense*) and canopy trees (*Beilschmiedia pendula*, *Priaria copaifera*, *Tetragastris panamensis*). All species with a significant effect had >200 individuals. Species with ~ 10 , ~ 100 , ~ 1000 and $\sim 10\,000$ individuals had CIs ± 0.37 , 0.34 , 0.24 and 0.08 of the mean, respectively. The posterior estimate of the community-wide mean of b (μ_b) was 0.14 , and the standard deviation (σ_b) was 0.19 . According to this fitted distribution of b , 78% of the species had higher mortality at higher light ($b > 0$), compared to 95% of direct estimates of individual species' b , a difference we attribute to sampling error.

The effect of log(dbh) on mortality was negative for all but one species (*Garcinia madruno*), with the parameter c ranging from -1.9 to 0.4 , (Fig. 1B; Supplementary material Appendix 2). For 276 species (97%), the effect of log(dbh) was significant. Species with ~ 10 , ~ 100 , ~ 1000 and $\sim 10\,000$ individuals had CIs $\pm 5.1\%$, 2.7% , 0.6% and 0.2% of the mean, respectively.

$\sim 10\,000$ individuals had CIs ± 0.75 , 0.63 , 0.47 and 0.21 of the mean, respectively. The community-wide mean of c (μ_c) was -1.0 , and the standard deviation (σ_c) was 0.4 . According to the fitted distribution of c , 99% of the species had $c < 0$.

The effect of dbh on mortality was positive for all but six species, with the parameter d ranging from -0.005 to 0.045 (Fig. 1C; Supplementary material Appendix 2). For 85 species (30%), the effect of dbh was significant. As d was negatively correlated with the maximum dbh of a species, the CI was wider for species with small maximum dbh than for species with large maximum dbh. The community-wide mean of d (μ_d) was 0.007 , and the standard deviation (σ_d) was 0.006 . According to the fitted distribution of d , 85% of the species had $d > 0$.

The effect of log(growth) on mortality was negative with the parameter e ranging from -0.53 to 0.06 (Fig. 1D; Supplementary material Appendix 2). For all but one species (*Garcinia madruno*), e was <0 , indicating lower mortality when trees grew faster. For 281 species (99%), the effect of growth was significant. Species with ~ 10 , ~ 100 , ~ 1000 and $\sim 10\,000$ individuals had CIs ± 0.23 , 0.20 , 0.14 and 0.04 of the mean, respectively. The community-wide mean of e (μ_e) was -0.35 , and the standard deviation (σ_e) was 0.12 . According to the fitted distribution of e , nearly all species (99.8%) had lower mortality when growing faster ($e < 0$).

Predicted annual mortality rate at 5% light, 5 cm dbh and 1 mm growth was strongly skewed to the right. Mean annual mortality was 3.1% (Fig. 2; Supplementary material Appendix 2), but varied widely between species, from 0.3% to 36% per year. Species with ~ 10 , ~ 100 , ~ 1000 and $\sim 10\,000$ individuals had CIs $\pm 5.1\%$, 2.7% , 0.6% and 0.2% of the mean, respectively.

Observed versus predicted mortality

In *Virola sebifera*, a midstory tree, mortality first decreased with increasing dbh and then increased again slightly towards

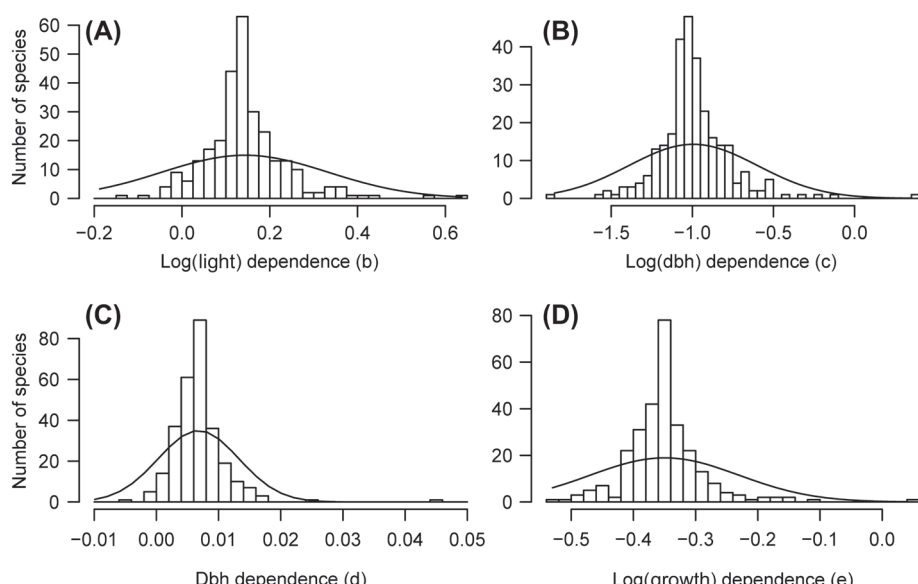


Figure 1. Species-specific means of the posterior distribution (histograms) and fitted hyperdistribution (lines) of the parameters of the mortality model; A the log(light) dependence of mortality (b), B log(dbh) dependence (c), C dbh dependence (d) and D log(growth) dependence (e) for 284 tree species at BCI, Panama.

the maximum dbh (Fig. 3A, D). Mortality was slightly higher at higher light (upper curve in Fig. 3A) and considerably higher at slow growth (upper curve in Fig. 3D). *Capparis frondosa*, an understory shrub, had decreasing mortality across its entire dbh range, and there was no effect of light on mortality (Fig. 3B) and only a slight effect of growth, especially in small trees (Fig. 3E). *Desmopsis panamensis*, an understory treelet, was one of the few species with increasing mortality across the entire dbh range. Mortality was significantly higher at higher light (Fig. 3C) and growth had a strong effect (Fig. 3F). Model fits for the remaining species are available as Supplementary material Appendix 3.

Contributions of light, size and growth to mortality

Increasing the light level by 1 SD (1.3%) for small trees of 1 cm dbh led to an increase of mortality in the average species from 12.2% to 12.8% per year, or a gain of 0.6 percentage points in mortality (Fig. 4A). At the extreme, though, some species showed 3 percentage point gains in mortality with 1 SD higher light. Increasing tree size from 1 cm to 2.5 cm dbh at average light (2%) decreased mortality, with the average impact of a decrease by 6.1 percentage points from 12.2% to 6.1% per year. There were species, though, which showed up to 30 percentage point declines. Past growth that was 1 SD faster than average resulted in a decrease of mortality by 2 percentage points on average, i.e. for an average species from 12.2% to 10.2% per year.

For larger trees of 10 cm dbh (Fig. 4B), increasing the light level by 1 SD (11%) led to an increase of mortality in the average species from 2.3% to 2.45% per year, or a gain of 0.15 percentage points in mortality. At the extreme, though, some species showed 2 percentage point gains with 1 SD higher light. Increasing tree size from 10 cm to 25 cm dbh at average light (18%) either decreased or increased mortality, with the average impact of an increase by 0.35 percentage points from 2.3% to 2.65% per year. There were species, though, which showed up to 10 percentage point increases or declines. Past growth that was 1 SD faster than average resulted in an average decrease of mortality by 0.4 percentage points, i.e. for an average species from 2.3% to 1.9% per year.

Species abundance and mortality responses

Across the community, the annual mortality at 5 cm dbh, 5% light and 1 mm growth decreased slightly with the

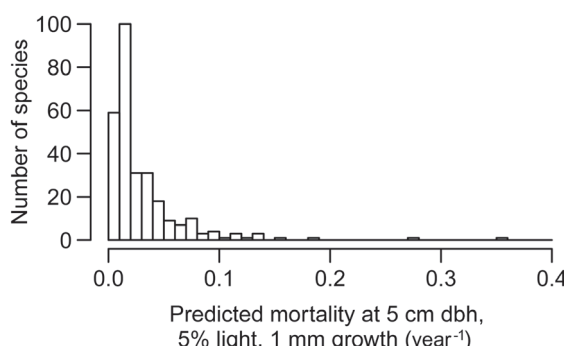


Figure 2. Predicted annual mortality rate at 5 cm dbh, 5% light and 1 mm growth per year for 284 tree species at BCI, Panama.

abundance of the species (Fig. 5). Posterior means of the impact of log(light) (b) and dbh (d) increased at higher abundances, whereas the effect of log(dbh) (c) and log(growth) (e) hardly changed with abundance. For species with <100 individuals, parameter estimates were partly determined by the community-wide mean. Therefore, the relationship of parameter estimates and abundance may not be informative for them.

Discussion

Almost 80% of the species had higher mortality at higher light. This light effect was significant for 29 out of 284 species, and for all of them mortality increased at higher light. These results challenge previous studies that found seedling and sapling mortality to decrease at higher light conditions (Augspurger 1984, Kobe 1999, de Souza and Válio 2001, Iriarte and Chazdon 2005, Aiba and Nakashizuka 2007, de Gouvenain et al. 2007). But these studies focussed on seedlings and very small saplings, and never included more than 15 species. The only study that also included trees >4 cm dbh focussed exclusively on species of the pioneer genus *Macaranga* and found lower mortality at higher crown exposure to light for four species and no effect in seven species (Davies 2001). In an earlier study of the BCI 50-ha plot, Welden et al. (1991) found higher mortality in gaps versus non-gaps for saplings (1–4 cm dbh). They attributed higher sapling mortality in gaps to stronger competition by the many small individuals and associated self-thinning and to mortality due to falling trees or limbs.

Two aspects related to mortality caused by tree or limb falls warrant consideration. Tree and limb falls may be more likely at the edges of gaps than in closed forest (Hubbell and Foster 1986, Aide 1987). This process would correctly be represented by a positive light effect because being located in a gap (i.e. at higher light levels) would increase the risk of mortality. It is also possible, however, to generate a false positive impact of high light, because saplings in deep shade killed by a tree fall from above would then (i.e. in the years of the census interval after their death) appear to be in light. We checked for this possibility by calculating the impact of light levels during the previous census interval on mortality and even more species (275 vs 269) had higher mortality in higher (prior) light. The community-wide mean was only 0.005 lower than when using current light. Thus, it appears that there is a real risk of living in an area of high light.

We hypothesise that lower seedling mortality at higher light found in some studies may be an artefact caused by the high sensitivity of seedling and sapling mortality to size. Seedlings in higher light environments grow faster (Poorter 1999). Thus, in the same study period seedlings in high light reach larger sizes than slower-growing individuals at lower light and consequently might have lower mortality due to their larger size rather than due to the higher light levels. Although it is not possible to control for changes in size during a mortality study, it is important to control for the initial size when impacts of light or other environmental conditions on mortality are to be evaluated.

Our results on the size dependence of mortality largely support previous studies. For the majority of tree species, mortality decreased steeply as small trees grew larger (Swaine 1989,

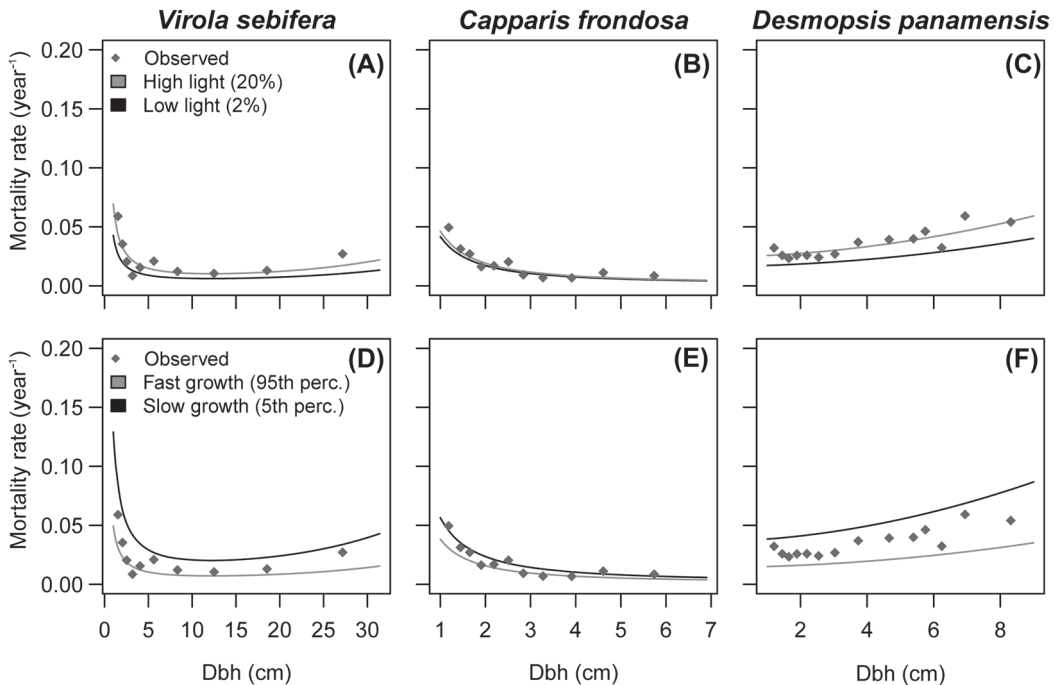


Figure 3. Predicted mortality at two light levels (2% and 20%, A–C) and two levels of growth (5th percentile and 95th percentile, D–F) for *Virola sebifera* ($n = 1654$), *Capparis frondosa* ($n = 2513$) and *Desmopsis panamensis* ($n = 4676$). In the upper panels, growth was fixed at mean growth of the species. In the lower panels, light was fixed at mean light available to the species. Dots represent observed mortality in ten dbh classes each containing a tenth of the individuals. For *Desmopsis*, the largest dbh class was split into another five classes each containing two percent of the individuals. The dbh range is restricted to 75% of the maximum dbh because larger trees are rare and model predictions become increasingly uncertain towards maximum dbh.

Turner 1990, Condit et al. 1995, Aiba and Nakashizuka 2007) and then either remained constant or increased again slightly towards the maximum diameter of the species (Davies 2001, King et al. 2006). Little is known about causes of mortality in tropical trees, but it is likely that saplings are more vulnerable to mechanical damage from above and possibly herbivory (Clark and Clark 1991, 1992). There is also evidence that both very small and the very biggest trees are more drought sensitive than intermediate sizes (Condit et al. 1995, Nakagawa et al. 2000). Indeed, a U-shaped mortality curve with age or size is so typical across all organisms that it is taken for granted.

The increase of mortality towards the maximum dbh appeared in many of the species at BCI, including shrubs (e.g. *Hybanthus prunifolius*), understory treelets (e.g. *Desmopsis panamensis*, *Farema occidentalis*), midstory trees (e.g. *Eugenia oerstediana*, *Guarea guidonia*, *Maquira guianensis*) and canopy trees (e.g. *Quararibea asterolepis*; Supplementary material Appendix 3). In other species, however, the increase in mortality at large dbh appears to have been an artefact of unbalanced data sets dominated by the many small individuals (e.g. *Inga marginata*, *Pterocarpus rohrii*, *Sympomia globulifera*, *Trichilia pallida*; Supplementary material Appendix 3). To account for unbalanced mortality data sets, semiparametric approaches have successfully been applied (Vieilledent et al. 2009). However, semiparametric approaches are not suitable for our study because they prevent a straightforward comparison among many species. Nevertheless, the model fits show that for the vast majority of species, mortality rates are well approximated at least up to a size of half the maximum dbh and this size range comprises about 90% of the individuals.

As expected from studies on temperate (Kobe et al. 1995, Wyckoff and Clark 2002, Wunder et al. 2008) and tropical forests (Swaine et al. 1987, Chao et al. 2008, Rozendaal et al. 2010), trees that were growing faster were consistently dying less often than slower-growing trees. This is easily interpreted as meaning that unhealthy trees tend to grow more slowly before dying, regardless of what factors contribute to poor health.

Of the factors we considered, tree size had the largest impact on mortality, followed by past growth and light availability. For small trees (1 cm dbh) this means that after the opening of a gap, potentially elevated mortality at higher light conditions is more than offset by the reduction of mortality due to the size increase allowed from the increase in light. Thus, mortality effectively decreases when a gap opens. For larger trees (10 cm dbh), further increase in dbh had varied impacts on mortality, with some species showing increase in mortality at large size, and others the opposite. Thus, pooling species with different maximum dbh can result in constant community-level mortality across different size classes as it has been found in many studies, obscuring intraspecific patterns (Lieberman and Lieberman 1987, Manokaran and Kochummen 1987, Swaine et al. 1987).

Uncertainty in our model fits comes from various sources: error in the light estimate, measurement error of past growth, sampling error in rare species, individual variability within species and other factors we did not study. Our light estimate obviously is only an approximate way of estimating the light environment in the forest. However, measuring light at every tree in the 50-ha plot would involve a prohibitive amount

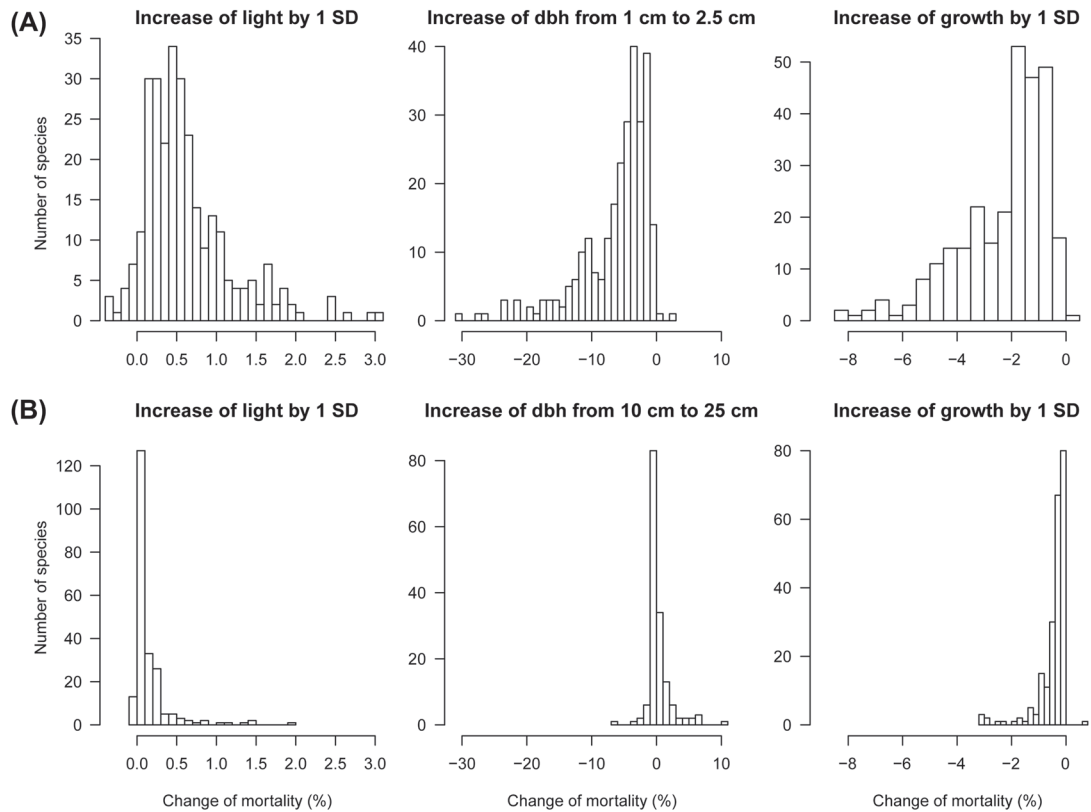


Figure 4. Contributions of light availability, size and growth to mortality. For small trees (A), contributions are expressed by the absolute difference in percentage points between baseline mortality of a tree at 1 cm dbh, average light (2%) and average growth ($0.35 \text{ mm year}^{-1}$) and mortality when light is increased by 1 SD to 3.3%, dbh is increased from 1 cm to 2.5 cm or growth that is 1 SD faster than average ($0.74 \text{ mm year}^{-1}$). For larger trees (B), contributions are expressed by the difference between baseline mortality of a tree at 10 cm dbh, average light (18%) and average growth (2 mm year^{-1}) and mortality when light is increased by 1 SD to 29%, dbh is increased from 10 cm to 25 cm or growth that is 1 SD faster than average (4.4 mm year^{-1}).

of time and labour. Until lidar-mapping data of the entire 50 ha are available, the method we propose offers an objective and straightforward measure of how much vegetation is blocking the sky above any tree of any height in the entire forest. In a previous study based on the same estimation of light availability, a strong impact of light on species-specific recruitment rates was detected (Rüger et al. 2009). This indicates that our light index captures relevant spatial heterogeneity of light availability.

A problem inherent in highly diverse tropical forests is the low number of individuals per area for the many rare species (Pitman et al. 1999). Hierarchical Bayesian methods explicitly account for this problem by superimposing a form of variation of the studied phenomenon across the community and by providing direct measures of uncertainty associated with parameter estimates (Clark 2005, Condit et al. 2006). We are aware that for species with few individuals it is difficult to separate the effects of our four predictors. While the average mortality rate could be estimated with low uncertainty for species with >100 individuals, >1000 individuals were needed to estimate the other model parameters with low uncertainty. Likewise, Wunder et al. (2008) report that growth dependence of mortality in virtual forests could only be reliably identified with inventory-based data for large sample sizes (>500 individuals). However, even if parameter estimates for any given species may be

associated with high uncertainty, the hierarchical approach ensures that the overall distribution of parameters across the community is described precisely, even for rare species.

Apart from tree size, light availability and past growth investigated in this study, other factors are known to influence mortality patterns, e.g. soil moisture and drought (Condit et al. 1995, Engelbrecht et al. 2006, Comita and Engelbrecht 2009), herbivory (Benítez-Malvido et al. 2005) or the number or basal area of conspecifics in the neighbourhood (Comita and Hubbell 2009, Comita et al. 2010). Thus, more detailed analyses of mortality rates may be worthwhile to reveal the contribution of these additional predictors to mortality. However, to do this, large data sets would be required that include observations of mortality for many individuals as well as measurements of several biotic and abiotic variables.

Conclusions

Mortality rates (at standardised conditions) of 284 woody tropical rainforest species at BCI, Panama, varied over a 100-fold range. This clearly indicates different life-history strategies and suggests mortality to be an important axis for species' classification into functional groups. Tree size was the most important determinant of mortality, followed by past

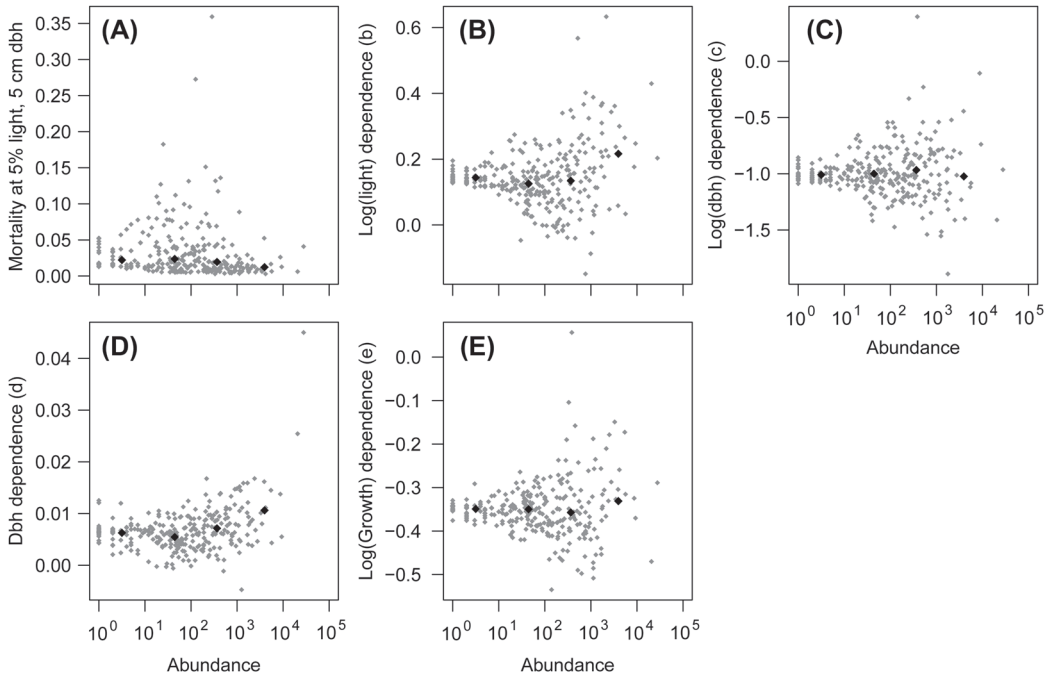


Figure 5. Posterior means of (A) the annual mortality rate at 5% light, 5 cm dbh and 1 mm growth ($1/(1+e^{-a})$), (B) the log(light) dependence of mortality (b), (C) log(dbh) dependence (c), (D) dbh dependence (d) and (E) log(growth) dependence (e) for 284 tree species at BCI, Panama, versus their abundance in 1990. Single species are represented by small grey dots, while averages for four abundance classes (1–10, 11–100, 101–1000, >1000) are shown with large black dots at average abundance within each class.

growth. The impact of light was comparatively low and thus, species-specific light dependence of mortality does not seem to be an important component of ecological differentiation and offers little scope for niche partitioning with respect to the resource light. Likewise, the explicit use of ‘low-light mortality’ in tradeoffs with other life-history traits is not supported by our results.

Acknowledgements – We thank Helene Muller-Landau for providing the step width adjusting routine of the Metropolis–Hastings algorithm and Jens Doleschal and the Center for Information Services and High Performance Computing, Technische Univ. Dresden, for the parallelisation of the R code and computing resources. NR was supported by a research grant from the Center for Tropical Forest Science, and RC by a fellowship from the National Center for Ecological Analysis and Synthesis (Santa Barbara, USA). The BCI plot has been made possible through the support of the US National Science Foundation, the John D. and Catherine D. McArthur Foundation, and the Smithsonian Tropical Research Institute. We thank the dozens of field assistants and botanists who have collected data on trees and carried out the canopy censuses in the BCI plot over the past 25 years.

References

- Aiba, M. and Nakashizuka, T. 2007. Variation in juvenile survival and related physiological traits among dipterocarp species co-existing in a Bornean forest. – *J. Veg. Sci.* 18: 379–388.
- Aide, T. M. 1987. Limbfalls – a major cause of sapling mortality for tropical forest plants. – *Biotropica* 19: 284–285.
- Akaike, H. 1974. A new look at the statistical model identification. – *IEEE Trans. Autom. Control* 19: 716–723.
- Augspurger, C. K. 1984. Seedling survival of tropical tree species: interactions of dispersal distance, light gaps and pathogens. – *Ecology* 65: 1705–1712.
- Benítez-Malvido, J. et al. 2005. Responses of seedling transplants to environmental variations in contrasting habitats of central Amazonia. – *J. Trop. Ecol.* 21: 397–406.
- Brokaw, N. V. L. 1985. Gap-phase regeneration in a tropical forest. – *Ecology* 66: 682–687.
- Chao, K. J. et al. 2008. Growth and wood density predict tree mortality in Amazon forests. – *J. Ecol.* 96: 281–292.
- Chave, J. et al. 2003. Spatial and temporal variation of biomass in a tropical forest: results from a large census plot in Panama. – *J. Ecol.* 91: 240–252.
- Clark, D. A. and Clark, D. B. 1992. Life history diversity of canopy and emergent trees in a neotropical rain forest. – *Ecol. Monogr.* 62: 315–344.
- Clark, D. B. and Clark, D. A. 1991. The impact of physical damage on canopy tree regeneration in tropical rain forests. – *J. Ecol.* 79: 447–457.
- Clark, J. S. 2005. Why environmental scientists are becoming Bayesians. – *Ecol. Lett.* 8: 2–14.
- Comita, L. S. and Engelbrecht, B. M. J. 2009. Seasonal and spatial variation in water availability drive habitat associations in a tropical forest. – *Ecology* 90: 2755–2765.
- Comita, L. S. and Hubbell, S. P. 2009. Local neighborhood and species’ shade tolerance influence survival in a diverse seedling bank. – *Ecology* 90: 328–334.
- Comita, L. S. et al. 2010. Asymmetric density dependence shapes abundances in a tropical tree community. – *Science* 329: 330–332.
- Condit, R. 1998. Tropical forest census plots. – Springer.
- Condit, R. et al. 1995. Mortality rates of 205 neotropical tree and shrub species and the impact of a severe drought. – *Ecol. Monogr.* 65: 419–439.

- Condit, R. et al. 2006. The importance of demographic niches to tree diversity. – *Science* 313: 98–101.
- Connell, J. H. et al. 1997. Subcanopy gaps in temperate and tropical forests. – *Aust. J. Ecol.* 22: 163–168.
- Davies, S. J. 2001. Tree mortality and growth in 11 sympatric *Macaranga* species in Borneo. – *Ecology* 82: 920–932.
- de Gouvenain, R. C. et al. 2007. Partitioning of understorey light and dry-season soil moisture gradients among seedlings of four rain-forest tree species in Madagascar. – *J. Trop. Ecol.* 23: 569–579.
- Denslow, J. S. 1987. Tropical rainforest gaps and tree species diversity. – *Annu. Rev. Ecol. Syst.* 18: 431–451.
- de Souza, R. P. and Válio, I. F. M. 2001. Seed size, seed germination, and seedling survival of Brazilian tropical tree species differing in successional status. – *Biotropica* 33: 447–457.
- Dupuy, J. M. and Chazdon, R. L. 2006. Effects of vegetation cover on seedling and sapling dynamics in secondary tropical wet forests in Costa Rica. – *J. Trop. Ecol.* 22: 65–76.
- Ellison, A. M. 2004. Bayesian inference in ecology. – *Ecol. Lett.* 7: 509–520.
- Engelbrecht, B. M. J. et al. 2006. Short dry spells in the wet season increase mortality of tropical pioneer seedlings. – *Oecologia* 148: 258–269.
- Foster, R. B. and Brokaw, N. V. 1982. Structure and history of the vegetation of Barro Colorado Island. – In: Leigh Jr., E. G. et al. (eds), *The ecology of a tropical forest: seasonal rhythms and long-term changes*. Smithsonian Inst., pp. 67–81.
- Gelman, A. et al. 1995. *Bayesian data analysis*. – Chapman and Hall.
- Hubbell, S. P. and Foster, R. B. 1983. Diversity of canopy trees in a neotropical forest and implications for conservation. – In: Sutton, S. L. et al. (eds), *Tropical rain forest: ecology and management*. Blackwell, pp. 25–41.
- Hubbell, S. P. and Foster, R. B. 1986. Canopy gaps and the dynamics of a neotropical forest. – In: Crawley, M. J. (ed.), *Plant ecology*. Blackwell, pp. 77–96.
- Iriarte Vivar Balderrama, S. and Chazdon, R. L. 2005. Light-dependent seedling survival and growth of four tree species in Costa Rican second-growth rain forests. – *J. Trop. Ecol.* 21: 383–395.
- King, D. A. et al. 2006. Growth and mortality are related to adult tree size in a Malaysian mixed dipterocarp forest. – *For. Ecol. Manage.* 223: 152–158.
- Kobe, R. K. 1999. Light gradient partitioning among tropical tree species through differential seedling mortality and growth. – *Ecology* 80: 187–201.
- Kobe, R. K. et al. 1995. Juvenile tree survivorship as a component of shade tolerance. – *Ecol. Appl.* 5: 517–532.
- Lieberman, D. and Lieberman, M. 1987. Forest tree growth and dynamics at La Selva, Costa Rica (1969–1982). – *J. Trop. Ecol.* 3: 347–358.
- Lieberman, M. et al. 1989. Forests are not just Swiss cheese – canopy stereogeometry of non-gaps in tropical forests. – *Ecology* 70: 550–552.
- Lieberman, M. et al. 1995. Canopy closure and the distribution of tropical forest tree species at La Selva, Costa Rica. – *J. Trop. Ecol.* 11: 161–177.
- Manokaran, N. and Kochummen, K. M. 1987. Recruitment, growth and mortality of tree species in a lowland dipterocarp forest in peninsular Malaysia. – *J. Trop. Ecol.* 3: 315–330.
- Metcalf, C. J. E. et al. 2009. A time to grow and a time to die: a new way to analyze the dynamics of size, light, age, and death of tropical trees. – *Ecology* 90: 2766–2778.
- Montgomery, R. A. and Chazdon, R. L. 2002. Light gradient partitioning by tropical tree seedlings in the absence of canopy gaps. – *Oecologia* 131: 165–174.
- Nakagawa, M. et al. 2000. Impact of a severe drought associated with the 1997–1998 El Niño in a tropical forest in Sarawak. – *J. Trop. Ecol.* 16: 355–367.
- Phillips, O. L. et al. 2004. Pattern and process in Amazon tree turnover, 1976–2001. – *Phil. Trans. R. Soc. B* 359: 381–407.
- Pitman, N. C. A. et al. 1999. Tree species distributions in an upper Amazonian forest. – *Ecology* 80: 2651–2662.
- Poorter, L. 1999. Growth responses of 15 rain-forest tree species to a light gradient: the relative importance of morphological and physiological traits. – *Funct. Ecol.* 13: 396–410.
- Poorter, L. and Kitajima, K. 2007. Carbohydrate storage and light requirements of tropical moist and dry forest tree species. – *Ecology* 88: 1000–1011.
- Purves, D. and Pacala, S. 2008. Predictive models of forest dynamics. – *Science* 320: 1452–1453.
- Rozendaal, D. M. A. et al. 2010. Tropical tree rings reveal preferential survival of fast-growing juveniles and increased juvenile growth rates over time. – *New Phytol.* 185: 759–769.
- Rüger, N. et al. 2009. Response of recruitment to light availability across a tropical lowland rainforest community. – *J. Ecol.* 97: 1360–1368.
- Swaine, M. D. 1989. Population dynamics of tree species in tropical forests. – In: Holm-Nielsen, L. B. et al. (eds), *Tropical forests: botanical dynamics, speciation and diversity*. Academic Press, pp. 101–110.
- Swaine, M. D. et al. 1987. Tree population dynamics at Kade, Ghana (1968–1982). – *J. Trop. Ecol.* 3: 331–345.
- Turner, I. M. 1990. Tree seedling growth and survival in a Malaysian rain forest. – *Biotropica* 22: 146–154.
- Vieilledent, G. et al. 2009. Biases in the estimation of size-dependent mortality models: advantages of a semiparametric approach. – *Can. J. For. Res.* 39: 1430–1443.
- Welden, C. W. et al. 1991. Sapling survival, growth, and recruitment – relationship to canopy height in a neotropical forest. – *Ecology* 72: 35–50.
- Windsor, D. M. et al. 1990. Características de la Precipitación de la Isla de Barro Colorado. – In: Rand, A. S. et al. (eds), *Ecología de un bosque tropical: ciclos estacionales y cambios a largo plazo*. Smithsonian Trop. Res. Inst., pp. 53–71.
- Wirth, R. et al. 2001. Spatial and temporal variability of canopy structure in a tropical moist forest. – *Acta Oecol.* 22: 235–244.
- Wunder, J. et al. 2008. Predicting tree mortality from growth data: how virtual ecologists can help real ecologists. – *J. Ecol.* 96: 174–187.
- Wyckoff, P. H. and Clark, J. S. 2002. The relationship between growth and mortality for seven co-occurring tree species in the southern Appalachian Mountains. – *J. Ecol.* 90: 604–615.

Supplementary material (available online as Appendix O19021 at <www.oikosoffice.lu.se/appendix>). Appendix 1–3.

Appendix 1

Calculation of the shading index using canopy density and conversion of the shading index to relative irradiance

1. Calculation of the shading index using canopy density

Consider an arbitrary point P whose three-dimensional coordinates in the forest are x, y, z , and consider a cell of vegetation C whose midpoint is at position x_c, y_c, z_c (Fig. A1). Call the horizontal distance between the two points d_c , calculated from x and y coordinates, and the vertical distance $h_c = z_c - z$. Assume the vegetation in the cell is a horizontal circle of radius r . Then the formula for the angle α_c of sky obscured by the layer of vegetation is

$$\alpha_c = \arctan\left(\frac{d_c + r}{h_c}\right) - \arctan\left(\frac{d_c - r}{h_c}\right) \text{ if } d_c \leq 20 \text{ m}$$

$$\alpha_c = 0 \text{ if } d_c > 20 \text{ m,}$$

as we assume vegetation further than 20 m away (horizontal distance) have no impact on the light reaching a point. We estimate the total shading at point P as

$$s_p = \sum_c \alpha_c,$$

where the summation means over all cells c in the 50-ha plot.

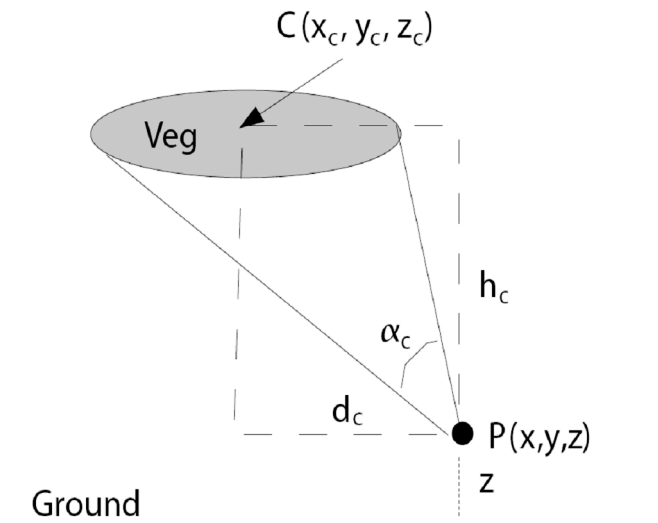


Figure A1: Diagram of the calculation converting vegetation density to shading. Point P at horizontal coordinates x, y , and height z , is where an estimate of shading is needed. The vegetation cell (Veg) has midpoint (vertical and horizontal) at point C . We assume the amount of light removed (*i.e.*, shading) by the vegetation cell is proportional to the angle α_c .

2. Conversion of the shading index to relative irradiance

We assumed a linear relationship between the log of relative irradiance l (data from Wirth *et al.* 2001) and the shading index s (for the period 1990–95) and performed a quadratic regression through 5th, 25th, 50th, 75th and 95th percentiles of both distributions, assuming that the lowest estimate of s for any tree individual (*a Prioria copaifera* tree with a dbh > 1.2 m) in any census interval corresponds to 100% light (Fig. A2). Thus, $l = e^{-0.01351-0.08043\cdot s-0.00315\cdot s^2}$. The distribution of estimated light is given in Fig. A3.

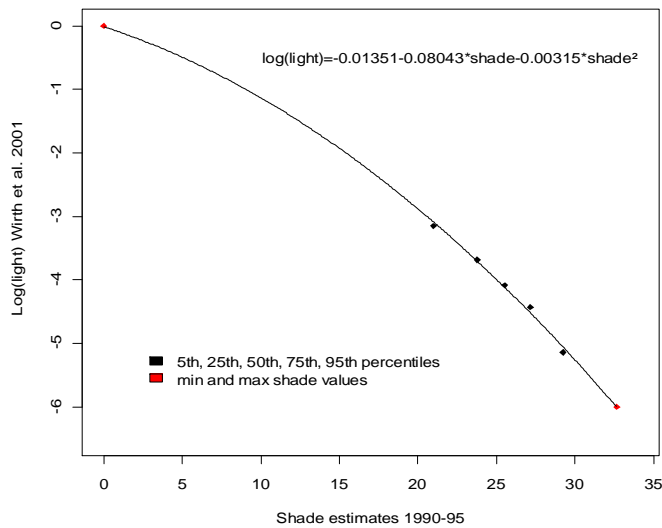


Figure A2: Conversion of shade estimates to relative irradiance.

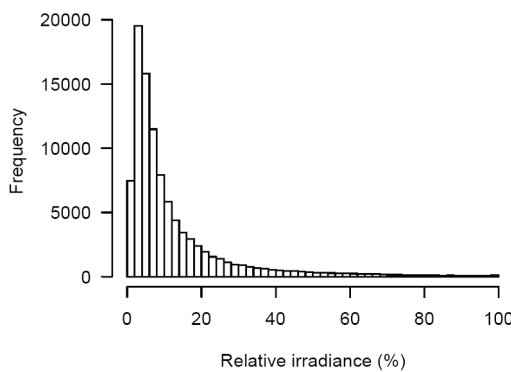


Figure A3: Distribution of estimated light for all individuals included in the analysis across the 50-ha plot on Barro Colorado Island, Panama.

References

- Wirth, R., Weber, B. & Ryel, R.J. (2001) Spatial and temporal variability of canopy structure in a tropical moist forest. *Acta Oecologica*, **22**, 235–244.

Species	Parameters														
	Constant (<i>a</i>)			Log(light) dependence (<i>b</i>)			Log(dbh) dependence (<i>c</i>)			Dbh dependence (<i>d</i>)			Log(growth) dependence (<i>e</i>)		
	mean	CI -	CI +	mean	CI -	CI +	mean	CI -	CI +	mean	CI -	CI +	mean	CI -	CI +
<i>Xylopia macrantha</i>	-5.21	-5.65	-4.76	0.248	-0.062	0.555	-1.15	-1.7	-0.56	0.0081	-0.001	0.0182	-0.408	-0.582	-0.225
<i>Xylosma oligandra</i>	-4.15	-4.83	-3.45	0.085	-0.228	0.469	-0.96	-1.58	-0.32	0.0067	-0.00418	0.02	-0.322	-0.538	-0.119
<i>Zanthoxylum acuminatum</i>	-3.34	-3.82	-2.83	0.138	-0.197	0.461	-0.59	-1.2	0.05	0.0108	0.00288	0.0197	-0.465	-0.662	-0.289
<i>Zanthoxylum ekmanii</i>	-0.98	-1.75	-0.1	0.04	-0.334	0.369	-1.24	-1.86	-0.6	0.0028	-0.00047	0.0061	-0.411	-0.586	-0.229
<i>Zanthoxylum panamense</i>	-3.35	-3.82	-2.87	-0.003	-0.328	0.331	-1.02	-1.59	-0.43	0.0091	0.00412	0.0144	-0.357	-0.537	-0.167
<i>Zanthoxylum setulosum</i>	-4.13	-6.02	-2.17	0.142	-0.242	0.511	-1.04	-1.84	-0.25	0.0048	-0.00542	0.0166	-0.344	-0.577	-0.114
<i>Zuelania guidonia</i>	-3.32	-4.24	-2.53	0.093	-0.244	0.463	-1.22	-1.92	-0.59	0.004	-0.00555	0.013	-0.354	-0.583	-0.142

Appendix 3

Comparison of observed and predicted mortality rates

We compared predicted and observed mortality rates in different ways for species with ≤ 100 or > 100 individuals, respectively. Mortality was recorded for the woody species at Barro Colorado Island, Panama, in the census interval 1990–1995. For species with < 100 individuals, overall observed and predicted mortality rate are reported (Table A2). To perform this comparison, we determined for each individual of a given species its predicted mortality based on the dbh, light and past growth of the individual.

For species with > 100 individuals, we visually compared predicted and observed mortality. We visualised the effect of light by drawing two curves of predicted mortality across the dbh range at 2% (black line) and 20% light (grey line), with growth fixed at mean growth of the species (Fig. A4). Likewise, we draw predicted mortality curves at slow growth (5th percentile, black line) and fast growth (95th percentile, grey line), with light fixed at mean light experienced by individuals of the species (Fig. A5).

The number of size classes depends on the abundance of the species. For species with > 100 and ≤ 1000 individuals, observed mortality rates were computed for three dbh classes each containing a third of the individuals (red dots). For species with > 1000 individuals, observed mortality rates were computed for ten dbh classes each containing a tenth of the individuals. Because large trees are rare, the largest dbh class can span half the dbh range. Thus, for species with > 2000 individuals, the largest dbh class was split into subclasses that contain at least 100 individuals. The dbh range is restricted to 75% of the maximum dbh because larger trees are rare and model predictions become increasingly uncertain towards maximum dbh.

The parameters of the mortality model are given in Appendix 2.

Table A2: Observed and predicted mortality rate for tree species with m_{100} individuals at Barro Colorado Island, Panama, in the census interval 1990–1995. N is the number of individuals alive in 1995.

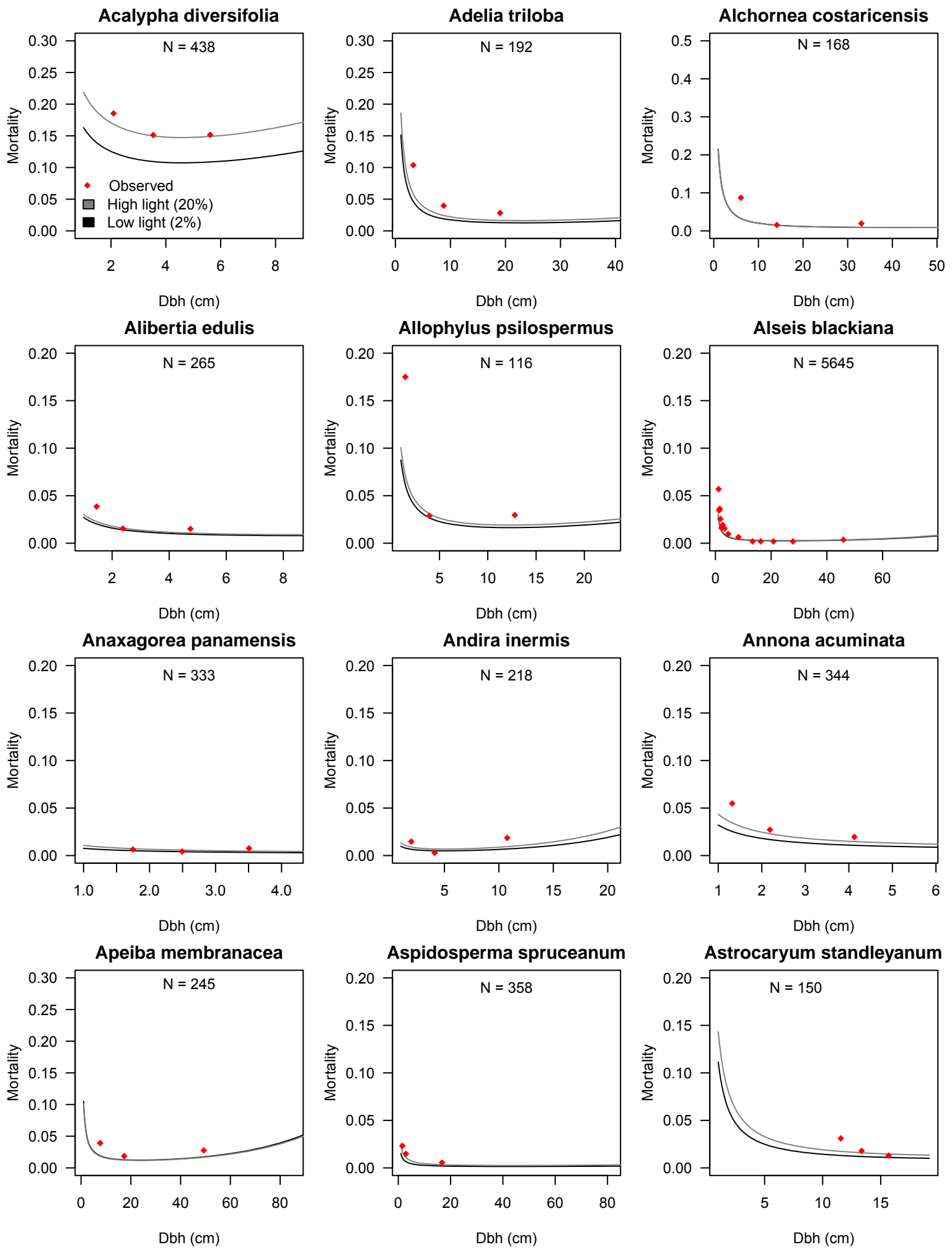
Species	Mortality		N
	Observed	Predicted	
<i>Abarema macradenia</i>	0.000	0.007	1
<i>Acacia melanoceras</i>	0.000	0.015	5
<i>Acalypha macrostachya</i>	0.144	0.117	20
<i>Aegiphila panamensis</i>	0.047	0.049	75
<i>Alchornea latifolia</i>	0.147	0.066	2
<i>Amaioua corymbosa</i>	0.032	0.033	14
<i>Anacardium excelsum</i>	0.000	0.003	12
<i>Annona spraguei</i>	0.072	0.087	41
<i>Apeiba tibourbou</i>	0.011	0.009	19
<i>Aphelandra sinclairiana</i>	0.000	0.023	4
<i>Appunia seibertii</i>	0.000	0.018	1
<i>Ardisia fendleri</i>	0.013	0.016	49
<i>Ardisia guianensis</i>	0.046	0.050	10
<i>Astronium graveolens</i>	0.000	0.003	50
<i>Attalea butyracea</i>	0.018	0.015	24
<i>Bactris barronis</i>	0.145	0.119	12
<i>Bactris coloniata</i>	0.231	0.200	18
<i>Bactris coloradonis</i>	0.229	0.116	3
<i>Bertiera guianensis</i>	0.000	0.053	1
<i>Brosimum guianense</i>	0.000	0.015	3
<i>Casearia commersoniana</i>	0.000	0.010	15
<i>Casearia guianensis</i>	0.018	0.022	12
<i>Cavanillesia platanifolia</i>	0.038	0.022	18
<i>Cecropia obtusifolia</i>	0.070	0.043	14
<i>Cedrela odorata</i>	0.000	0.006	1
<i>Ceiba pentandra</i>	0.067	0.063	29
<i>Cespedesia spathulata</i>	0.085	0.057	3
<i>Cestrum megalophyllum</i>	0.208	0.216	89
<i>Chamaedorea tepejilote</i>	0.231	0.182	9
<i>Chimarrhis parviflora</i>	0.000	0.018	3
<i>Chrysophyllum cainito</i>	0.016	0.018	54
<i>Cinnamomum triplinerve</i>	0.054	0.052	48
<i>Clidemia dentata</i>	1.000	0.077	1
<i>Cojoba rufescens</i>	0.000	0.014	1
<i>Colubrina glandulosa</i>	0.000	0.009	1
<i>Conostegia bracteata</i>	1.000	0.041	1
<i>Conostegia cinnamomea</i>	0.207	0.207	94
<i>Cordia alliodora</i>	0.034	0.040	79
<i>Coutarea hexandra</i>	0.000	0.017	2
<i>Cupania cinerea</i>	0.107	0.068	5
<i>Cupania latifolia</i>	0.045	0.050	36
<i>Cupania rufescens</i>	0.037	0.035	43
<i>Diospyros artanthifolia</i>	0.011	0.013	40
<i>Dipteryx oleifera</i>	0.011	0.014	39
<i>Elaeis oleifera</i>	0.000	0.004	7
<i>Enterolobium schomburgkii</i>	0.000	0.010	12
<i>Erythroxylum panamense</i>	0.042	0.043	76
<i>Ficus bullenei</i>	1.000	0.216	1
<i>Ficus colubrinae</i>	0.000	0.027	1
<i>Ficus insipida</i>	0.085	0.040	3

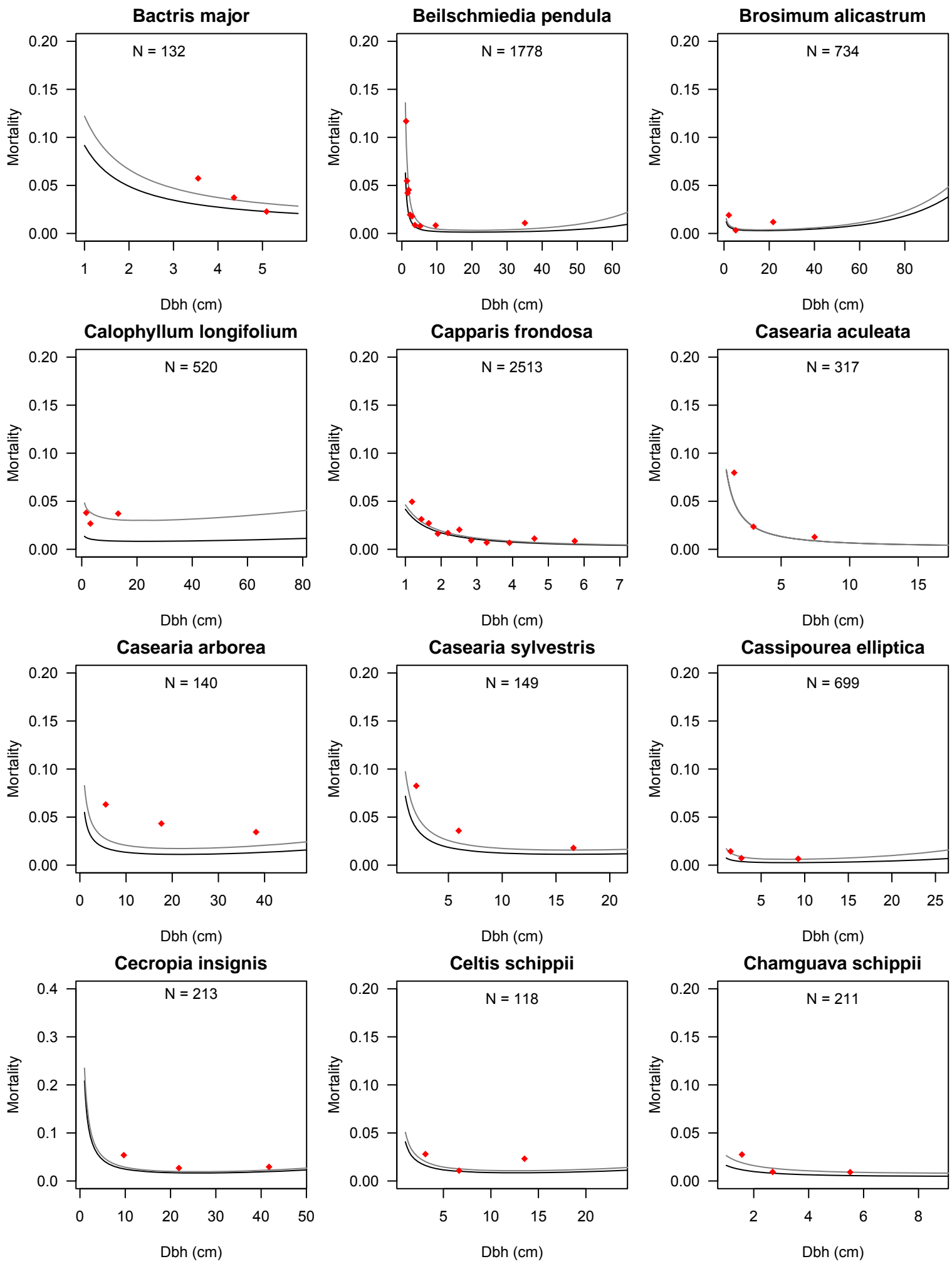
Table 3.1: continued

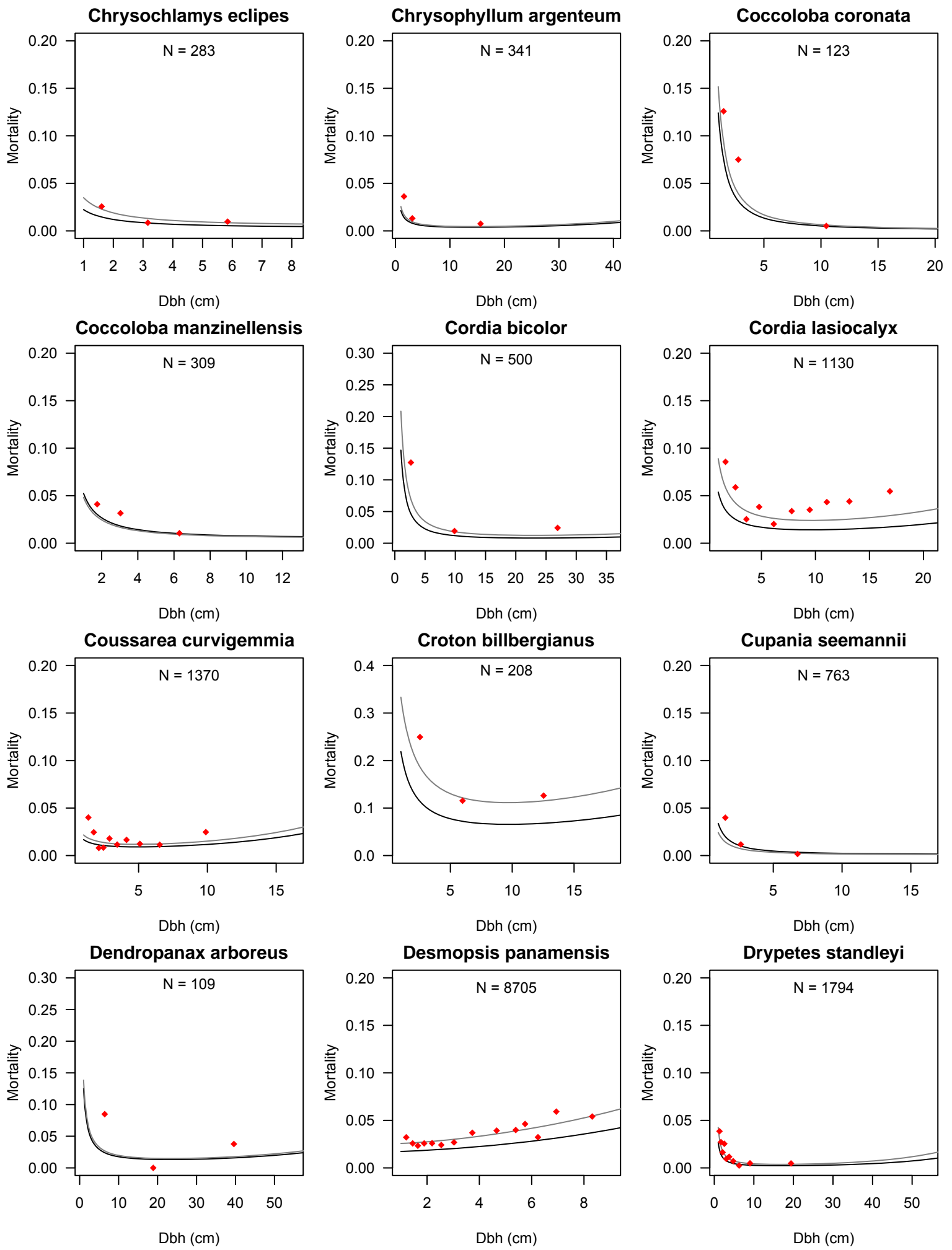
<i>Ficus maxima</i>	0.000	0.009	5
<i>Ficus obtusifolia</i>	0.000	0.008	1
<i>Ficus popenoei</i>	0.085	0.055	3
<i>Ficus tonduzii</i>	0.039	0.034	35
<i>Ficus trigonata</i>	0.000	0.005	2
<i>Ficus yoponensis</i>	0.000	0.007	2
<i>Genipa americana</i>	0.031	0.031	72
<i>Geonoma interrupta</i>	1.000	0.111	1
<i>Guarea grandifolia</i>	0.020	0.021	43
<i>Guazuma ulmifolia</i>	0.038	0.035	30
<i>Hamelia axillaris</i>	0.119	0.118	30
<i>Hamelia patens</i>	0.144	0.056	2
<i>Hampea appendiculata</i>	0.145	0.120	22
<i>Heisteria acuminata</i>	0.018	0.018	84
<i>Hieronyma alchorneoides</i>	0.030	0.032	68
<i>Hirtella americana</i>	0.037	0.035	31
<i>Hura crepitans</i>	0.012	0.013	89
<i>Inga cocleensis</i>	0.110	0.110	61
<i>Inga laurina</i>	0.036	0.037	50
<i>Inga mucuna</i>	0.000	0.031	1
<i>Inga oerstediana</i>	0.192	0.109	5
<i>Inga punctata</i>	0.146	0.129	12
<i>Inga ruiziana</i>	0.092	0.079	17
<i>Inga spectabilis</i>	0.052	0.042	18
<i>Inga thibaudiana</i>	0.034	0.034	53
<i>Koanophyllum wetmorei</i>	0.096	0.061	8
<i>Lacistema panamensis</i>	0.003	0.005	77
<i>Laetia procera</i>	0.032	0.029	21
<i>Lafoensia punicifolia</i>	0.000	0.005	7
<i>Lindackeria laurina</i>	0.016	0.014	55
<i>Lozania pittieri</i>	0.143	0.063	2
<i>Maclura tinctoria</i>	0.000	0.008	1
<i>Macrocnemum roseum</i>	0.026	0.028	61
<i>Malpighia romeroana</i>	0.042	0.044	44
<i>Margaritaria nobilis</i>	0.000	0.014	4
<i>Marila laxiflora</i>	0.000	0.014	1
<i>Maytenus schippii</i>	0.009	0.012	68
<i>Miconia elata</i>	0.060	0.053	20
<i>Miconia hondurensis</i>	0.000	0.007	23
<i>Miconia impetiolaris</i>	0.039	0.029	6
<i>Miconia nervosa</i>	0.226	0.227	71
<i>Myrcia gatunensis</i>	0.058	0.061	37
<i>Myrsinaceae frutescens</i>	0.078	0.062	13
<i>Nectandra fuzzy</i>	0.145	0.053	4
<i>Nectandra lineata</i>	0.083	0.083	49
<i>Nectandra purpurea</i>	0.035	0.034	39
<i>Neea amplifolia</i>	0.100	0.100	37
<i>Ochroma pyramidalis</i>	0.000	0.003	5
<i>Ocotea oblonga</i>	0.090	0.092	80
<i>Ormosia amazonica</i>	0.000	0.020	2
<i>Ormosia coccinea</i>	0.005	0.008	45
<i>Ormosia macrocalyx</i>	0.015	0.019	58
<i>Pachira sessilis</i>	0.022	0.023	20
<i>Piper aequale</i>	0.156	0.158	36
<i>Piper arboreum</i>	0.104	0.096	33

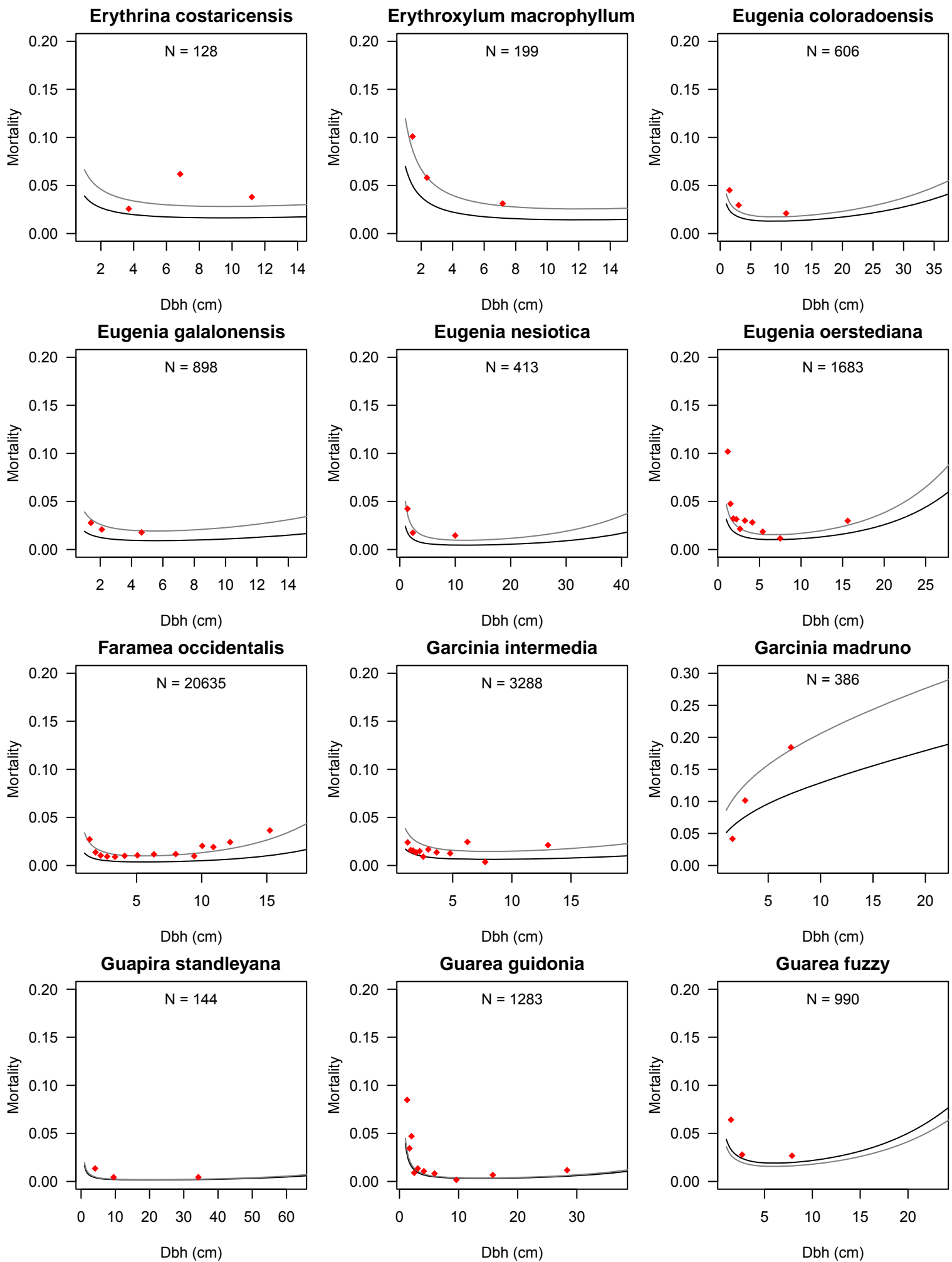
Table 3.1: continued

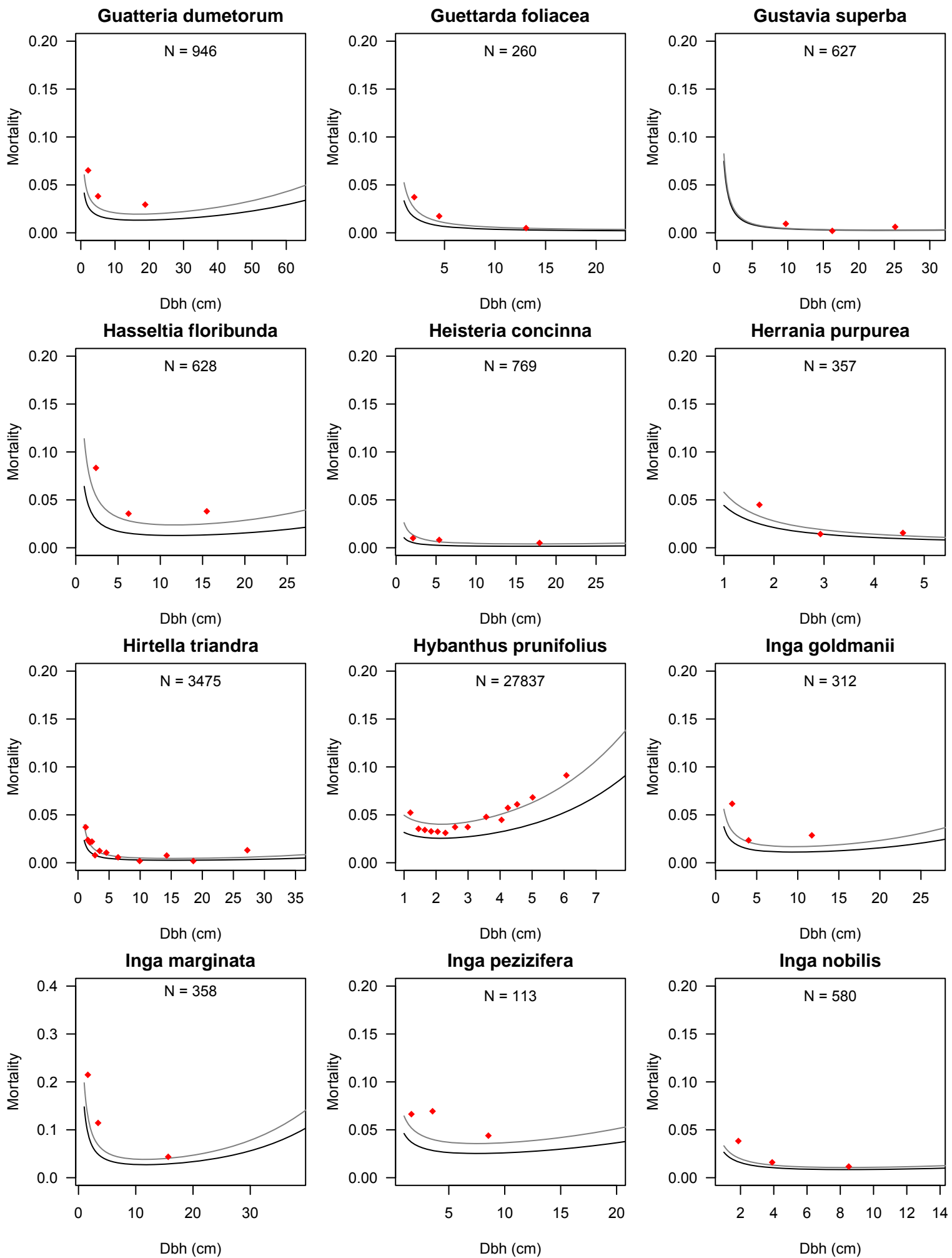
<i>Piper colonense</i>	0.132	0.123	34
<i>Piper perlasense</i>	0.135	0.135	42
<i>Piper reticulatum</i>	0.018	0.017	87
<i>Piper schiedeanum</i>	0.146	0.108	2
<i>Platymiscium pinnatum</i>	0.094	0.049	100
<i>Platypodium elegans</i>	0.054	0.058	97
<i>Posoqueria latifolia</i>	0.014	0.016	62
<i>Pourouma bicolor</i>	0.009	0.010	24
<i>Pouteria fossilcola</i>	0.000	0.020	2
<i>Pouteria stipitata</i>	0.009	0.010	49
<i>Protium confusum</i>	0.000	0.014	2
<i>Pseudobombax septenatum</i>	0.000	0.008	5
<i>Psidium friedrichsthalianum</i>	0.012	0.016	35
<i>Psychotria acuminata</i>	1.000	0.076	1
<i>Psychotria chagrensis</i>	0.070	0.071	7
<i>Psychotria deflexa</i>	0.305	0.285	26
<i>Psychotria graciliflora</i>	0.204	0.182	8
<i>Psychotria grandis</i>	0.090	0.092	43
<i>Psychotria limonensis</i>	0.146	0.124	2
<i>Psychotria pittieri</i>	0.000	0.065	1
<i>Psychotria tenuifolia</i>	0.000	0.034	1
<i>Pterocarpus officinalis</i>	0.000	0.023	4
<i>Quassia amara</i>	0.009	0.010	97
<i>Rosenbergiodendron formosum</i>	0.000	0.022	2
<i>Sapium broadleaf</i>	0.000	0.007	2
<i>Sapium glandulosum</i>	0.047	0.035	20
<i>Schizolobium parahyba</i>	0.000	0.009	10
<i>Senna dariensis</i>	0.196	0.218	46
<i>Siparuna guianensis</i>	0.000	0.007	18
<i>Solanum circinatum</i>	1.000	0.040	1
<i>Solanum hayesii</i>	0.173	0.150	25
<i>Solanum steyermarkii</i>	0.142	0.071	2
<i>Spachea membranacea</i>	0.000	0.025	1
<i>Spondias mombin</i>	0.041	0.038	39
<i>Sterculia apetala</i>	0.019	0.017	35
<i>Tabebuia guayacan</i>	0.008	0.010	54
<i>Terminalia amazonia</i>	0.018	0.019	48
<i>Terminalia oblonga</i>	0.031	0.028	66
<i>Tetrathylacium johansenii</i>	0.000	0.004	4
<i>Theobroma cacao</i>	0.015	0.014	15
<i>Thevetia ahouai</i>	0.053	0.055	63
<i>Tocoyena pittieri</i>	0.046	0.106	5
<i>Trattinnickia aspera</i>	0.055	0.052	65
<i>Trema micrantha</i>	0.175	0.111	7
<i>Trichanthera gigantea</i>	0.107	0.069	5
<i>Trichospermum galeottii</i>	1.000	0.350	1
<i>Turpinia occidentalis</i>	0.030	0.035	68
<i>Virola multiflora</i>	0.021	0.023	43
<i>Vismia baccifera</i>	0.060	0.054	40
<i>Vismia billbergiana</i>	0.149	0.052	2
<i>Vochysia ferruginea</i>	0.060	0.051	20
<i>Xylosma oligandra</i>	0.051	0.034	100
<i>Zanthoxylum setulosum</i>	0.000	0.022	1
<i>Zuelania guidonia</i>	0.060	0.061	28

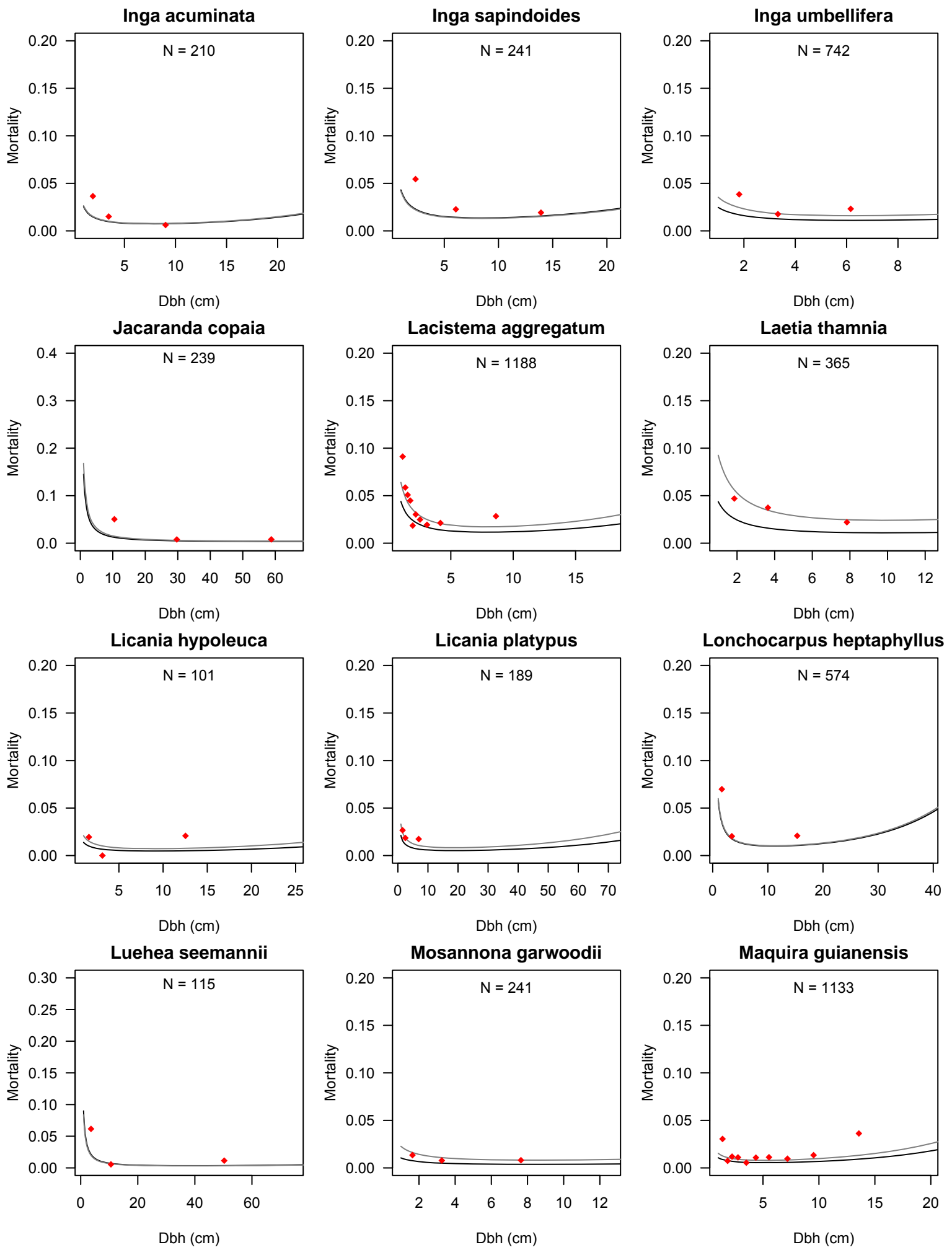


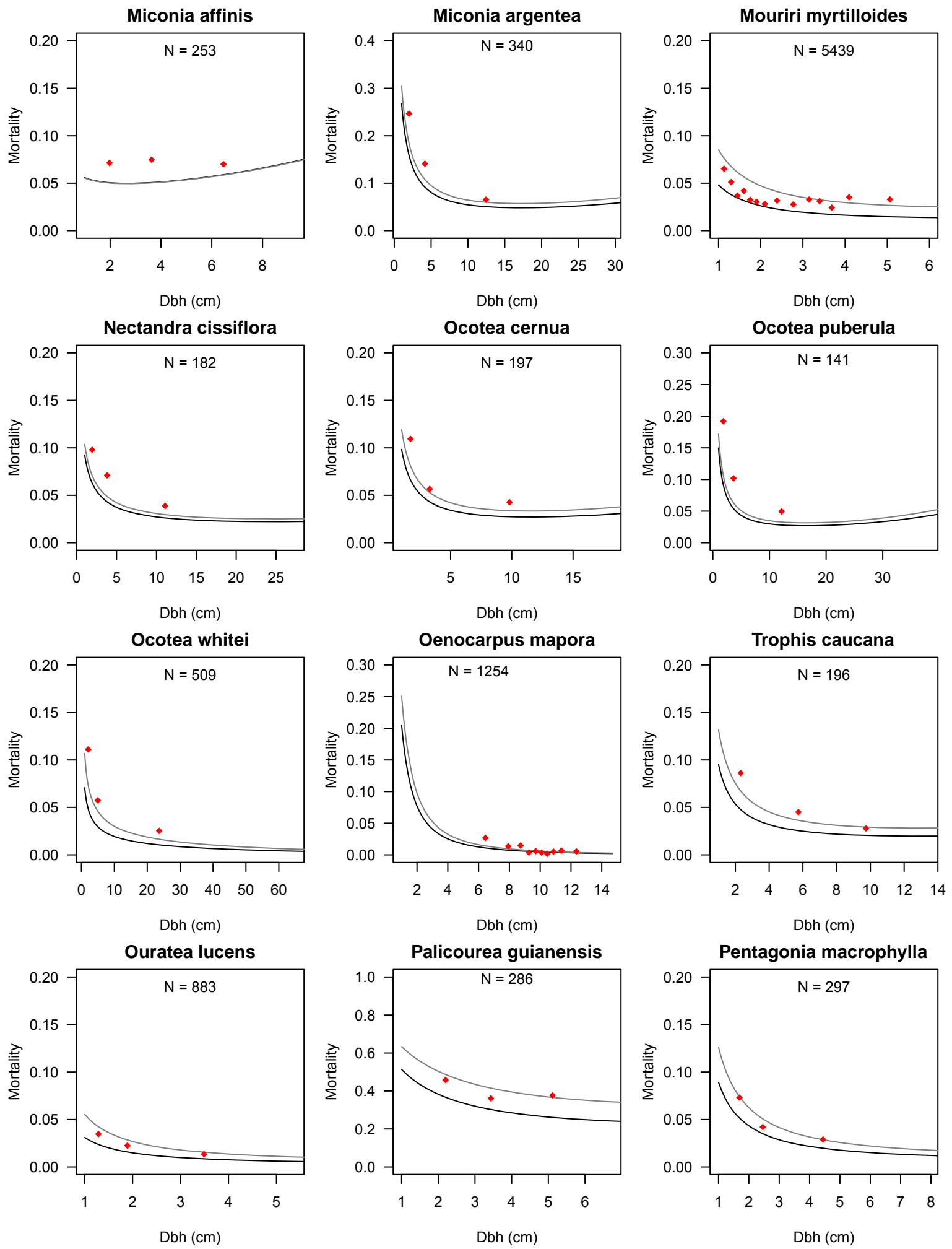


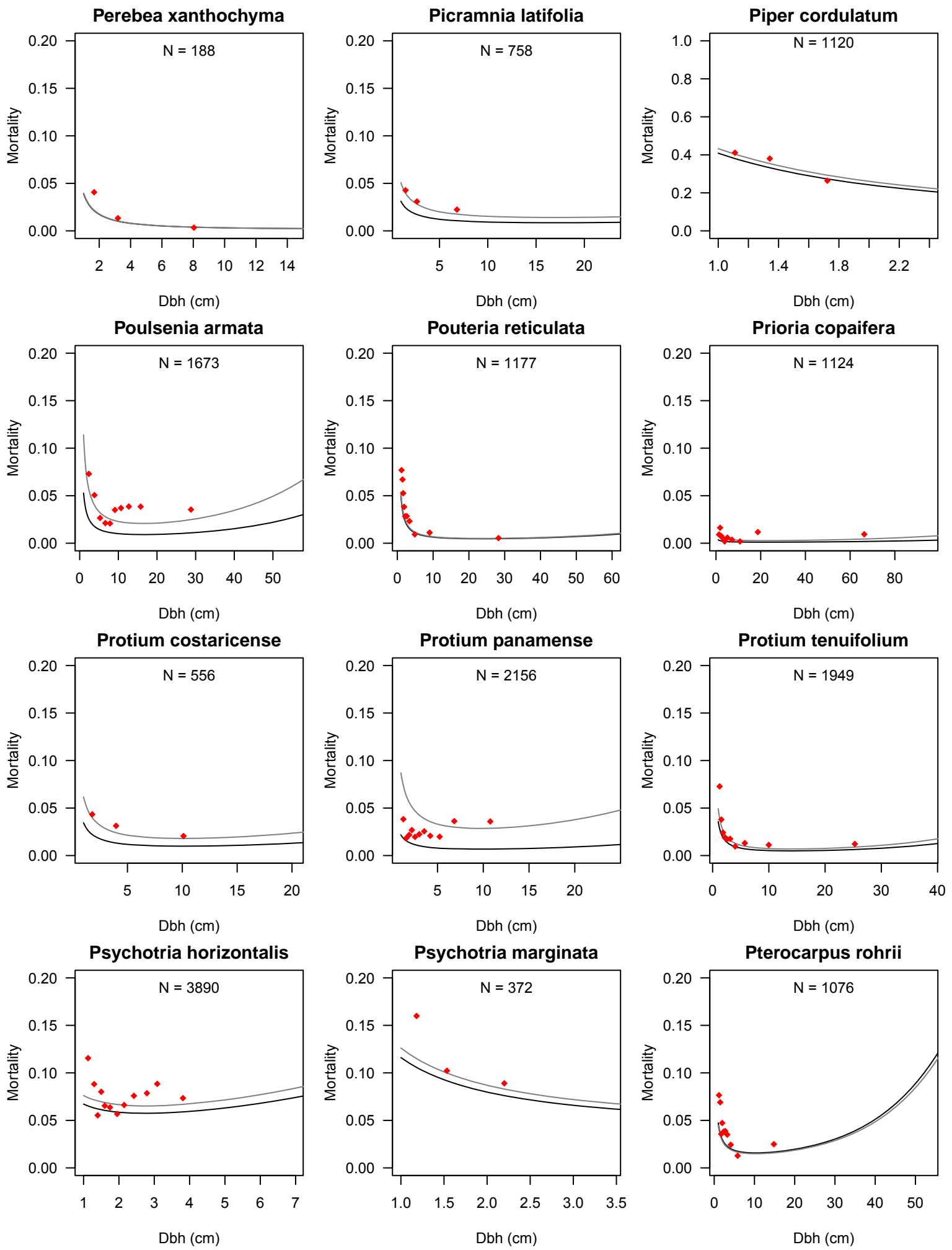


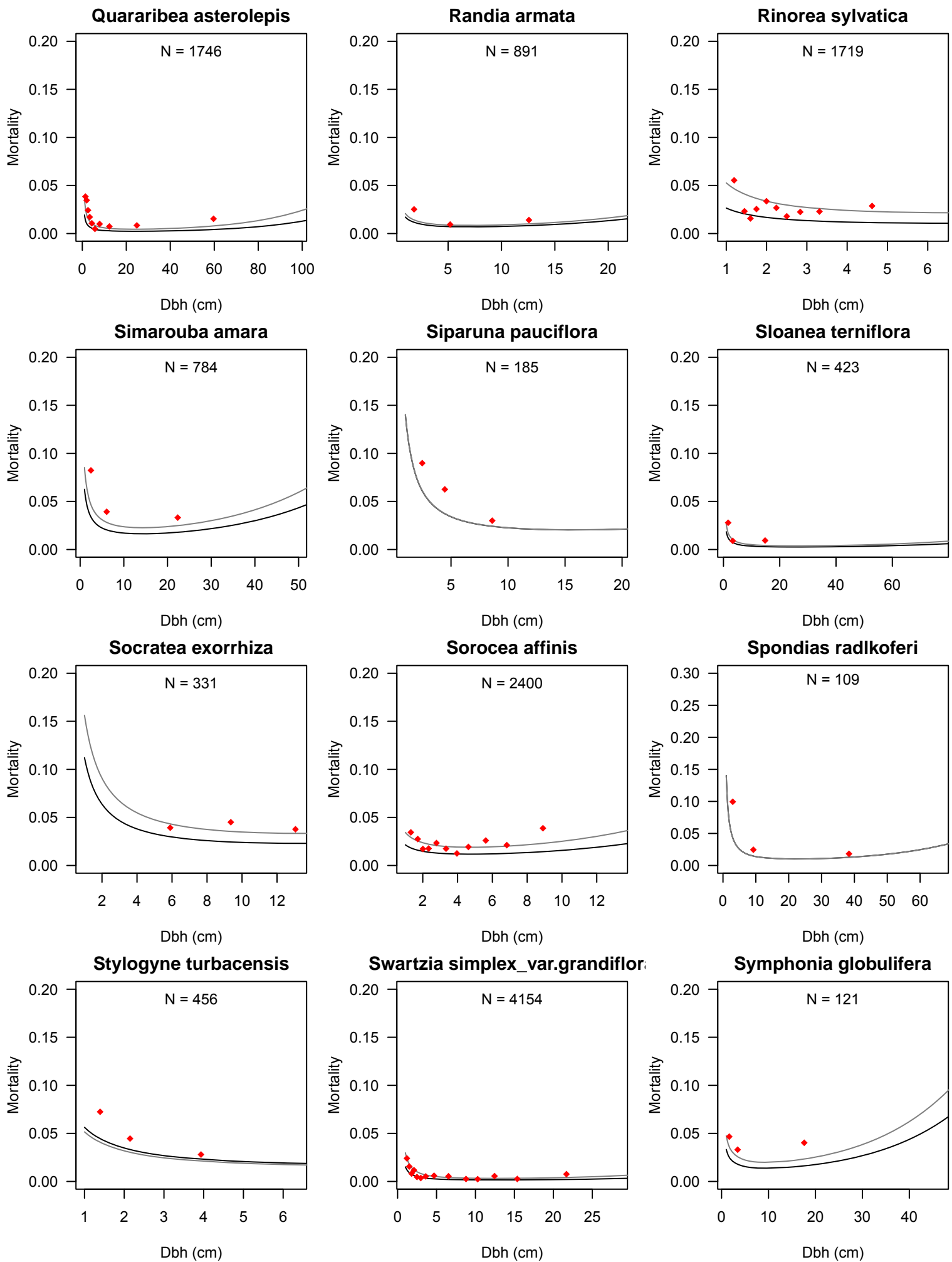


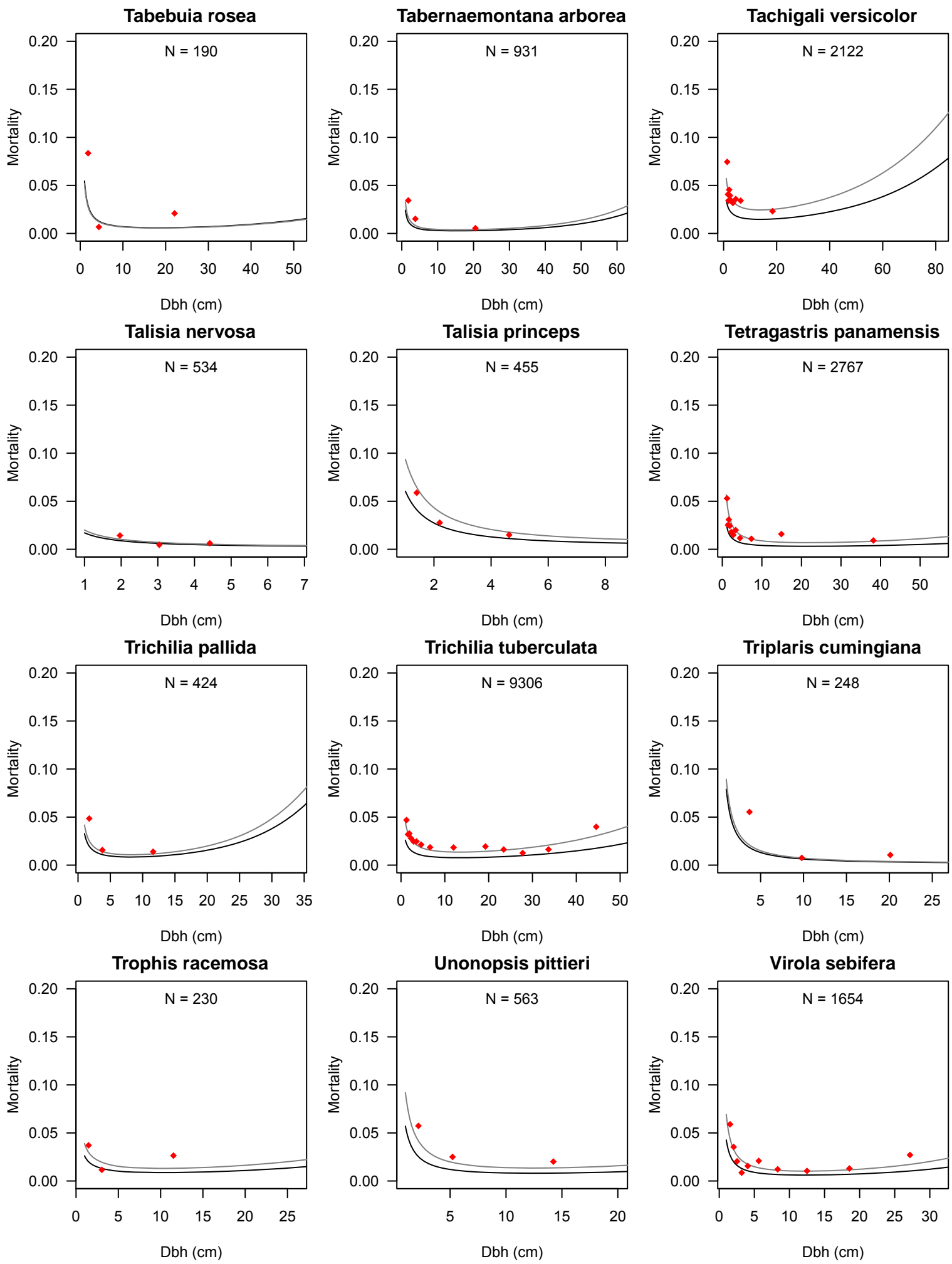


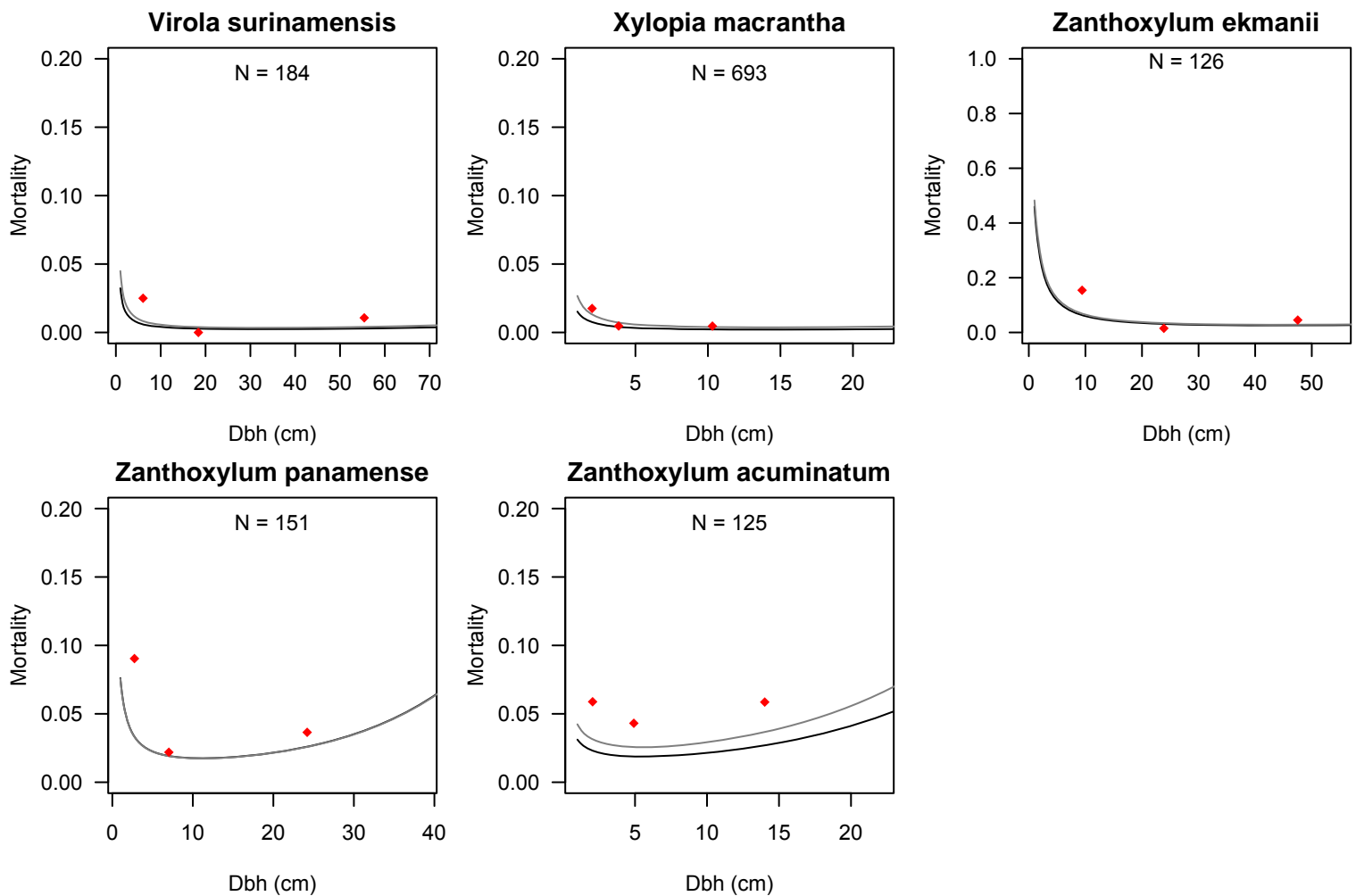


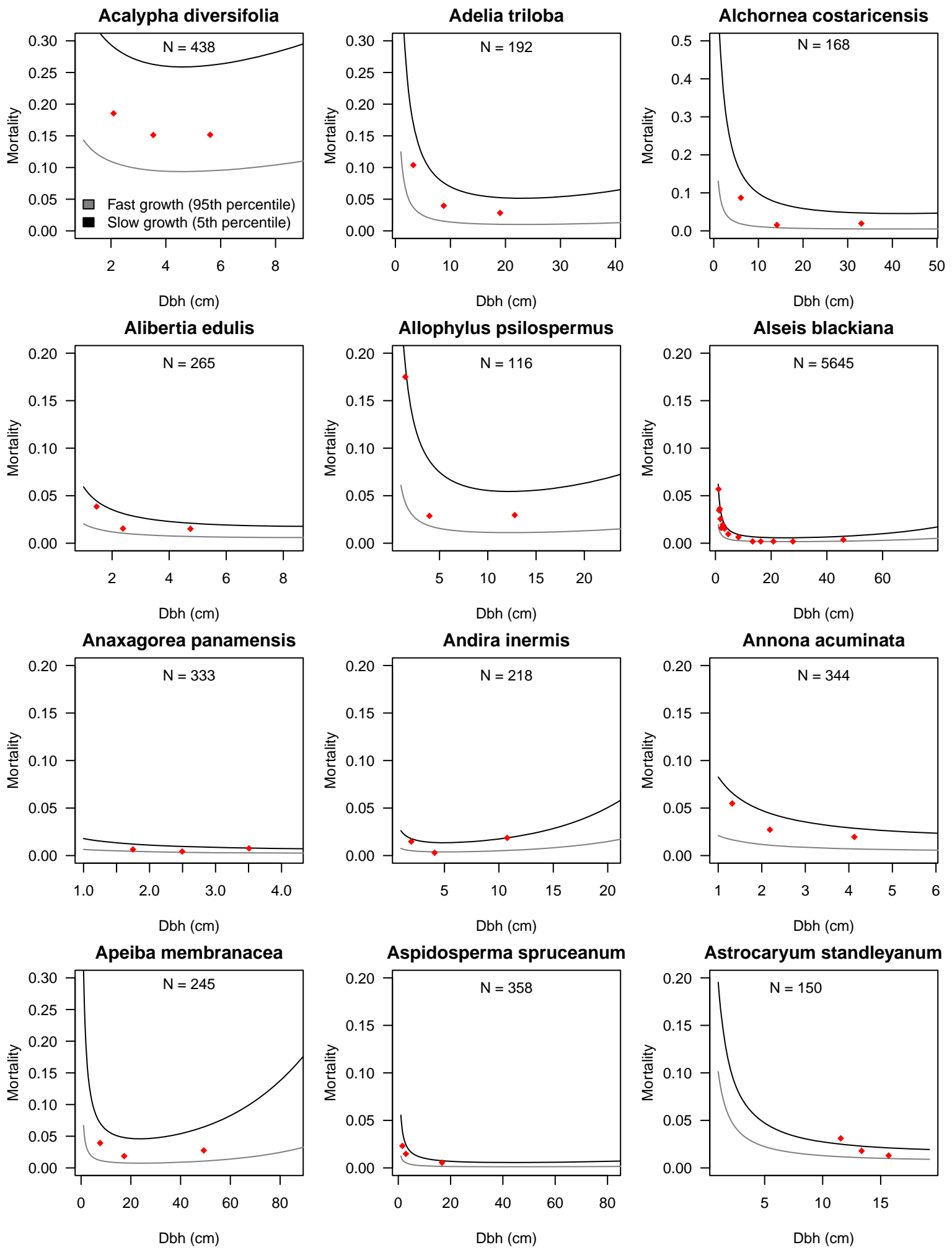


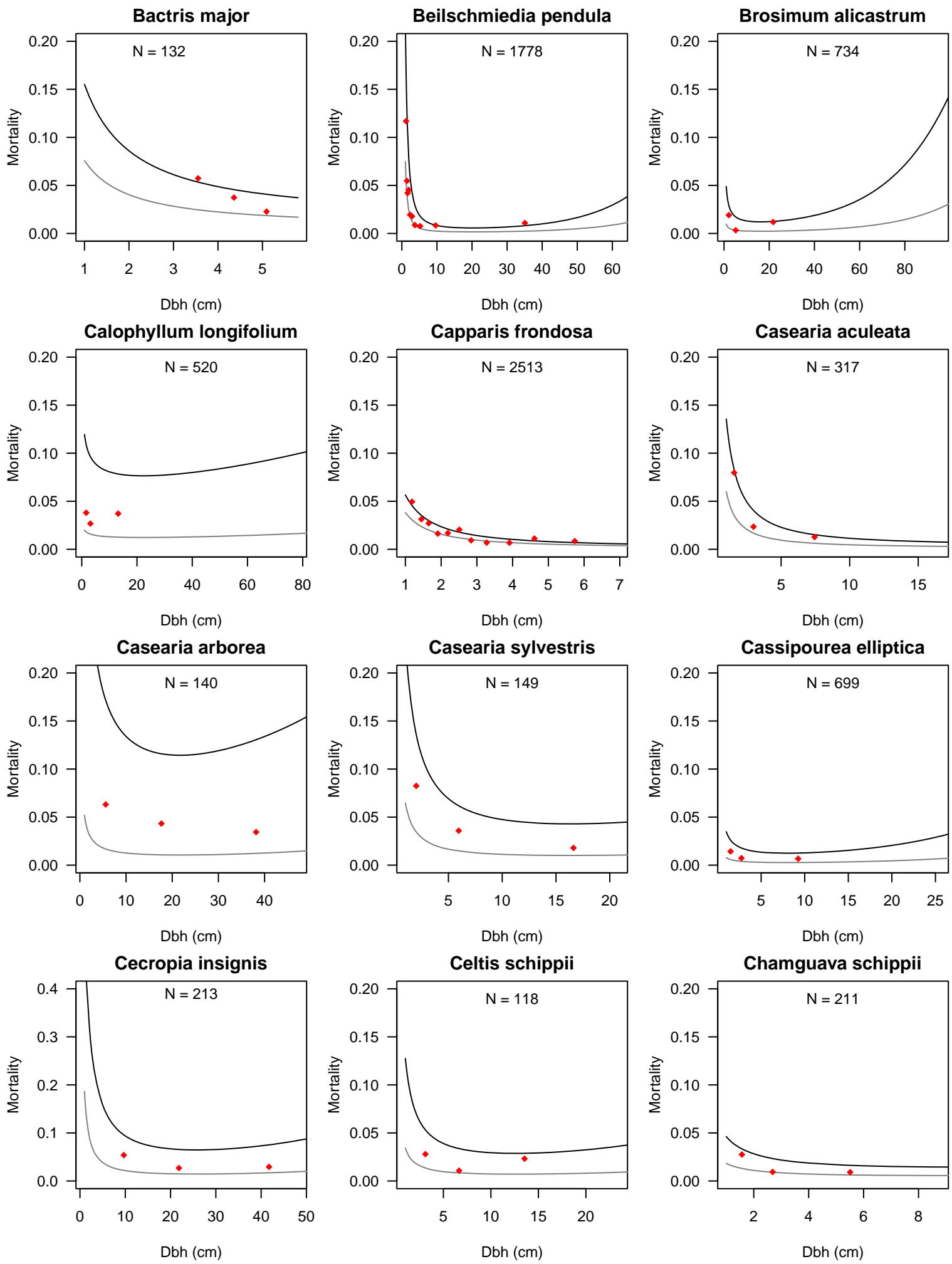


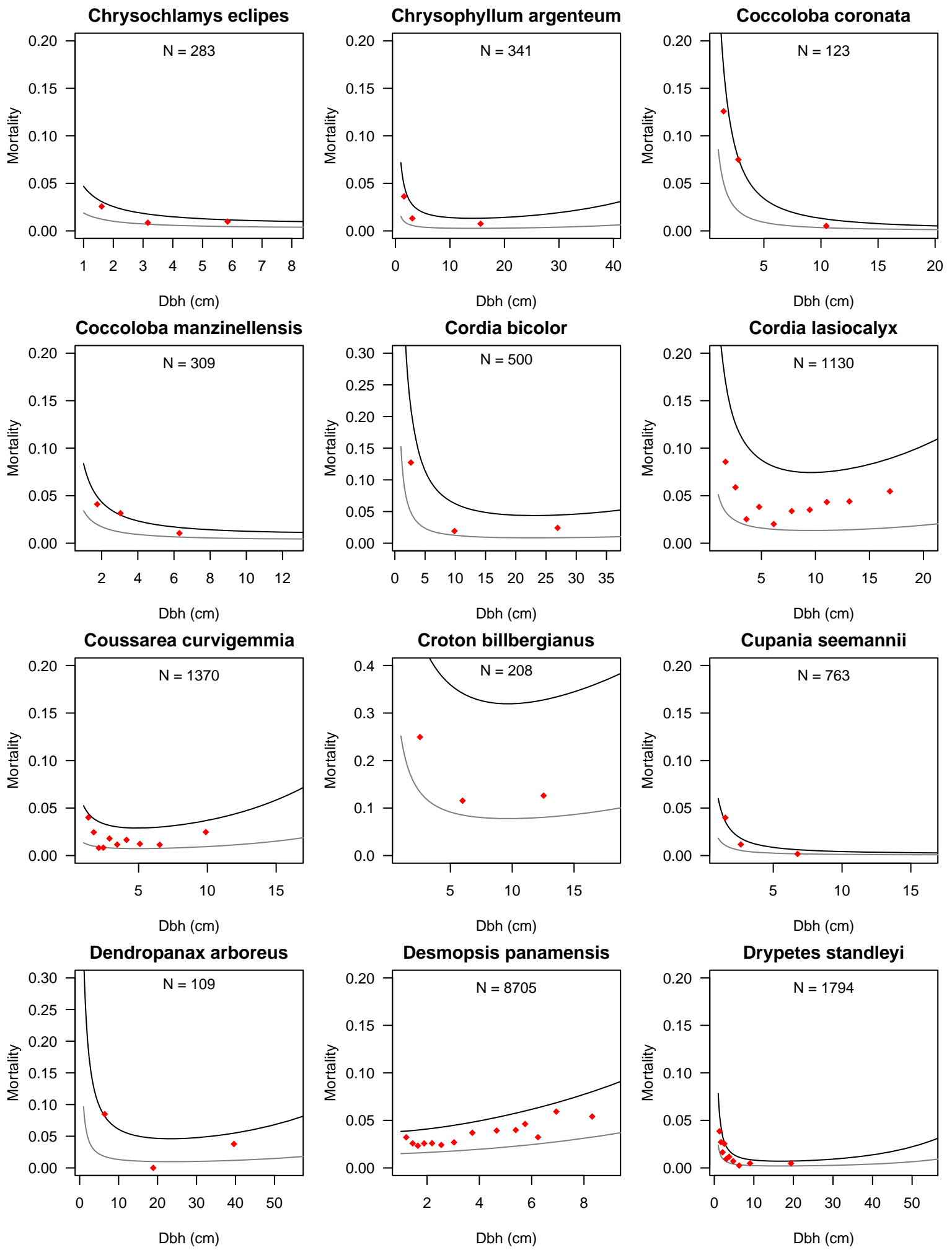


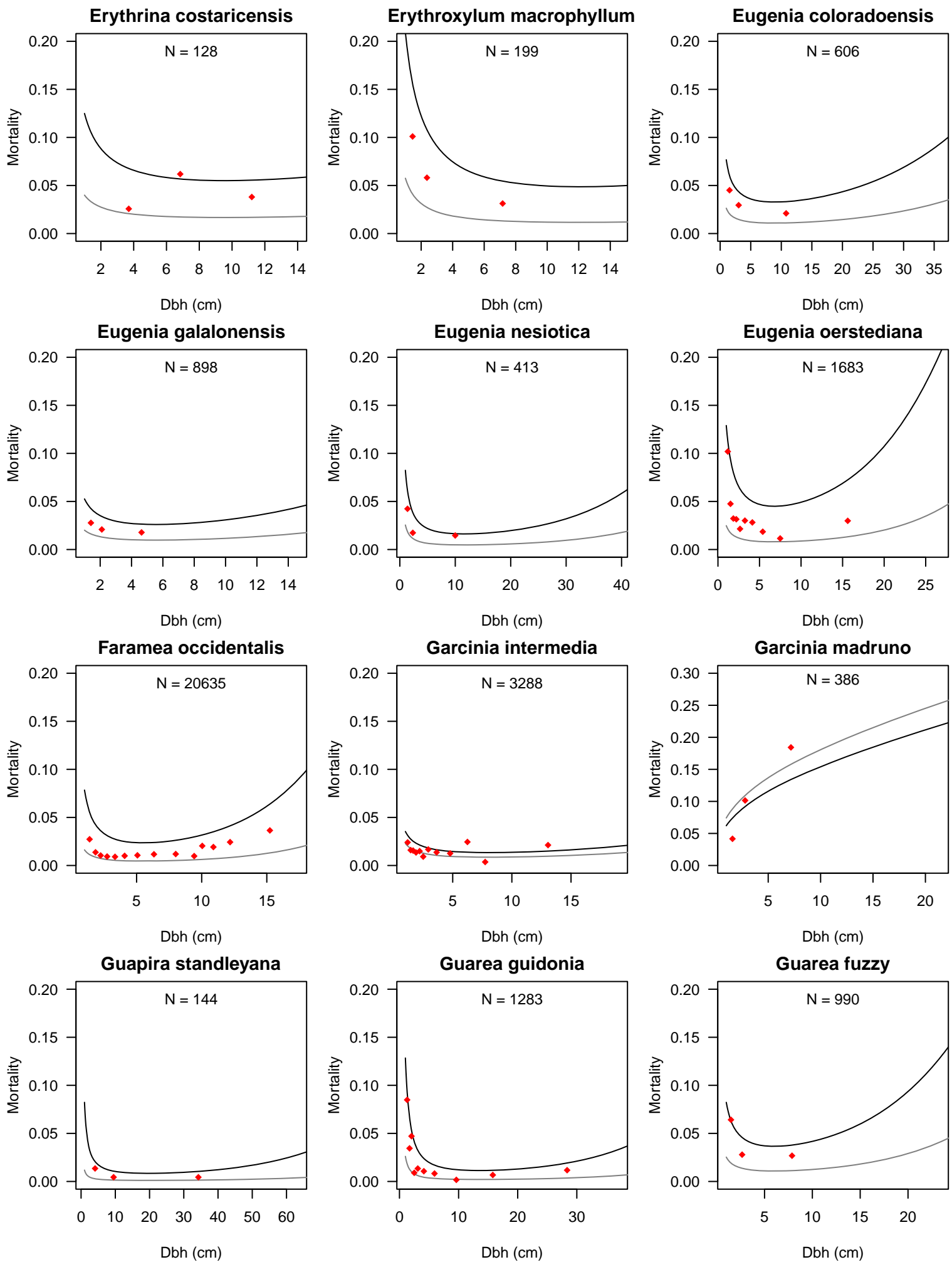


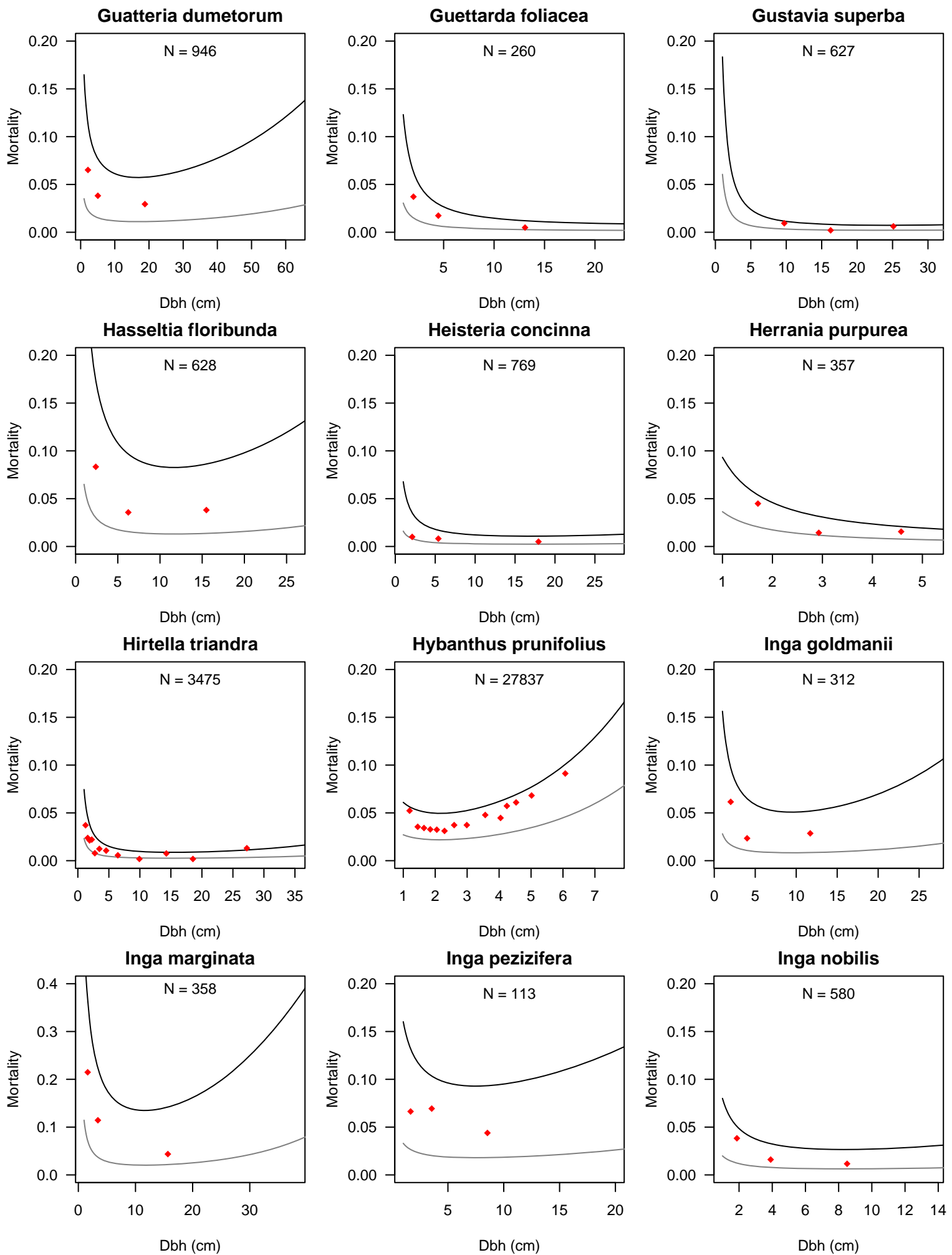


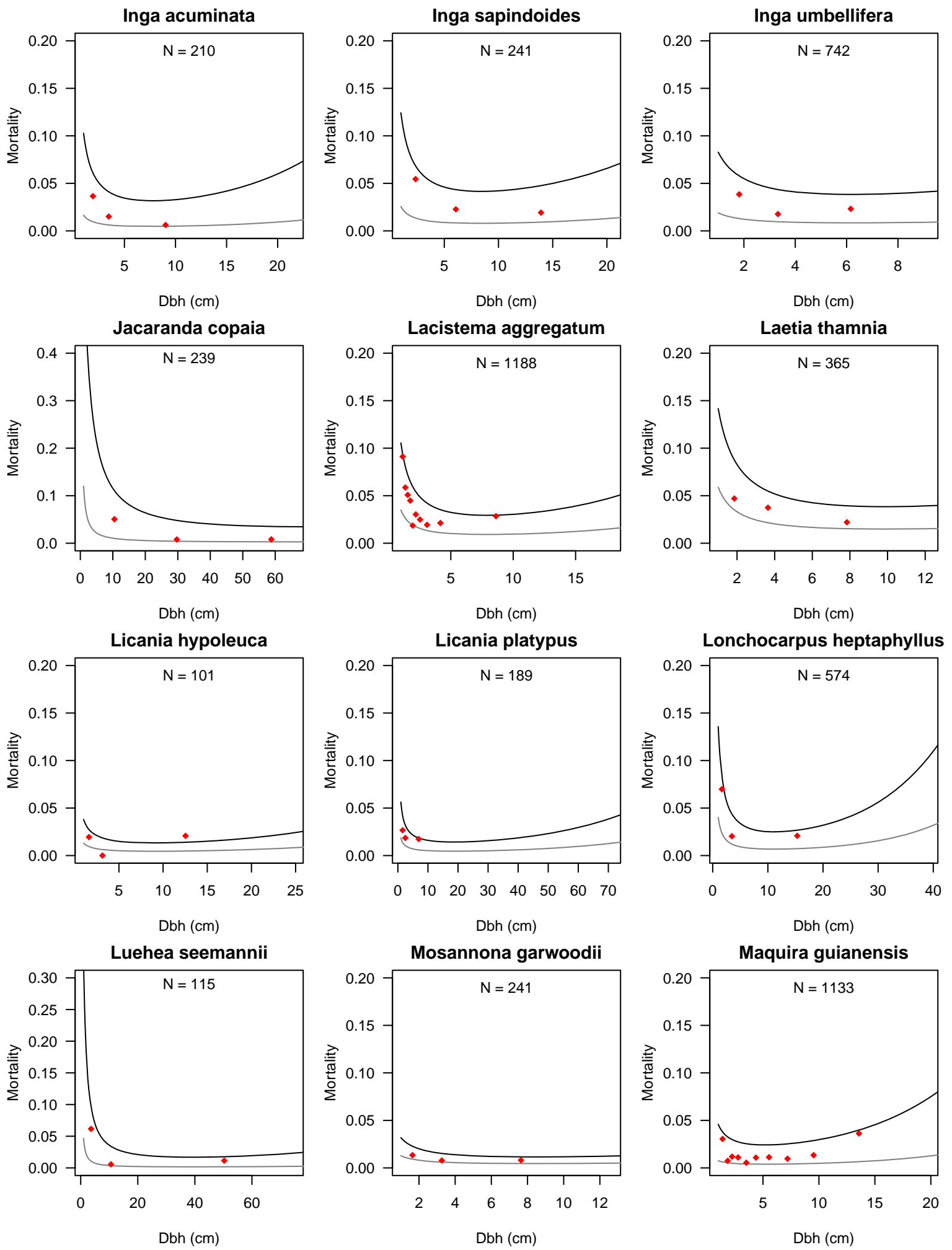


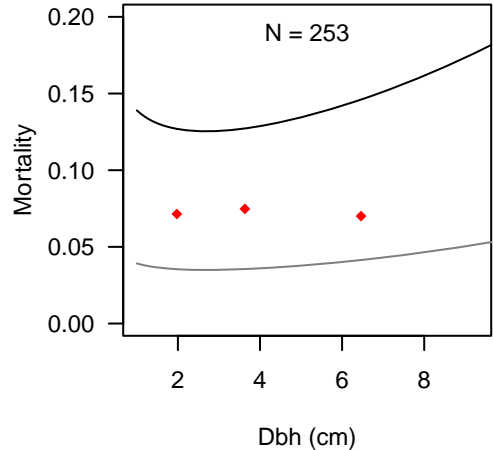
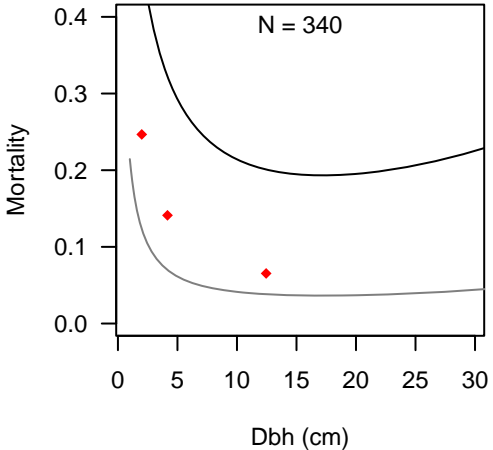
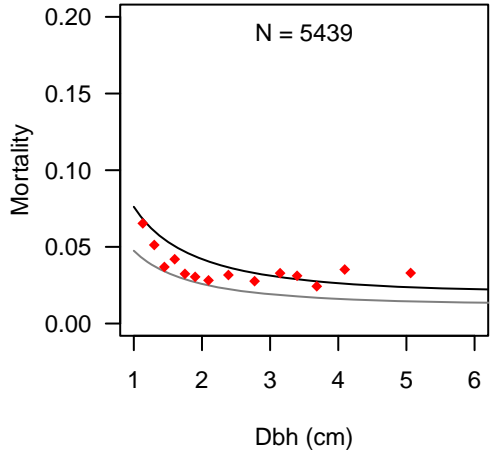
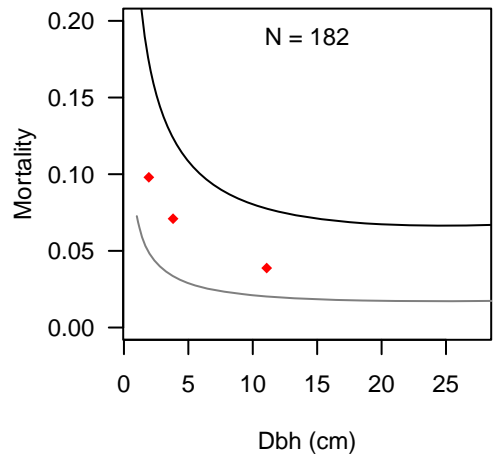
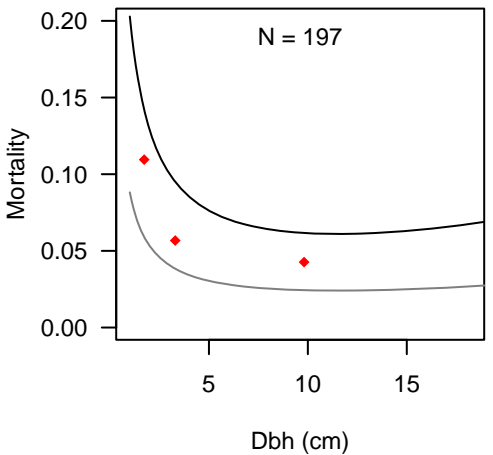
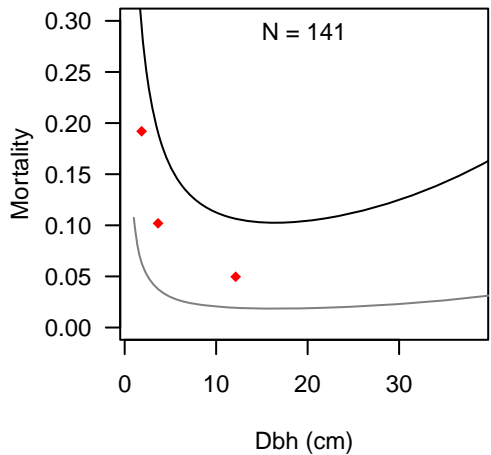
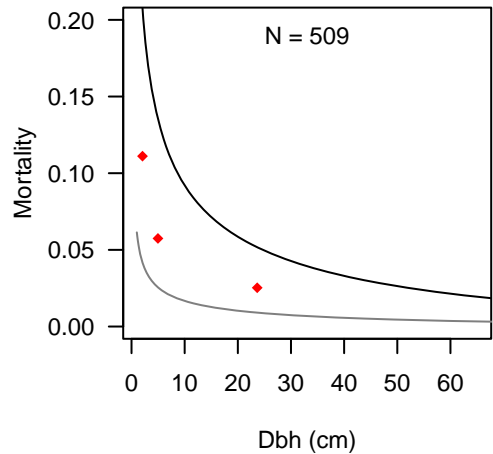
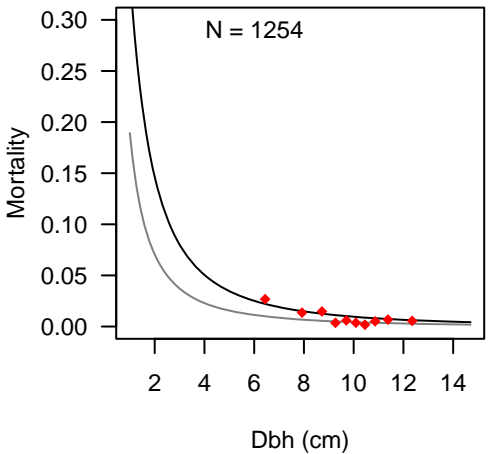
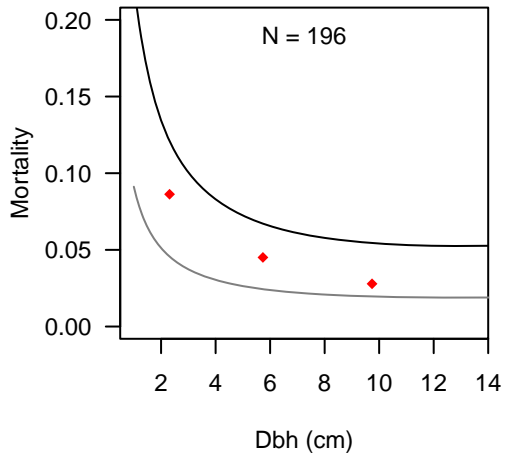
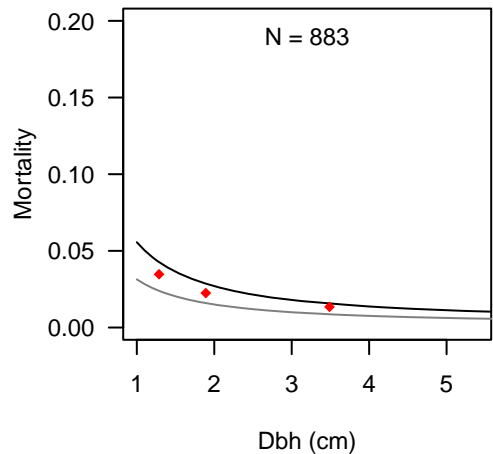
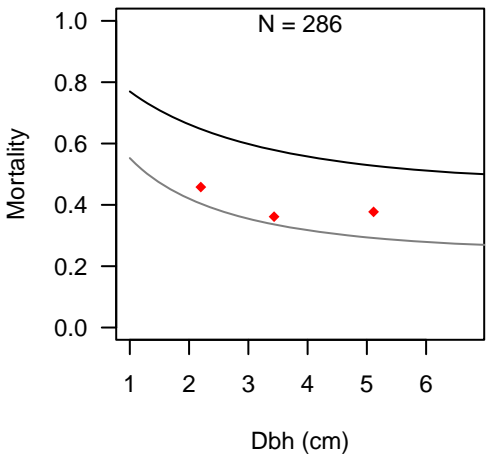
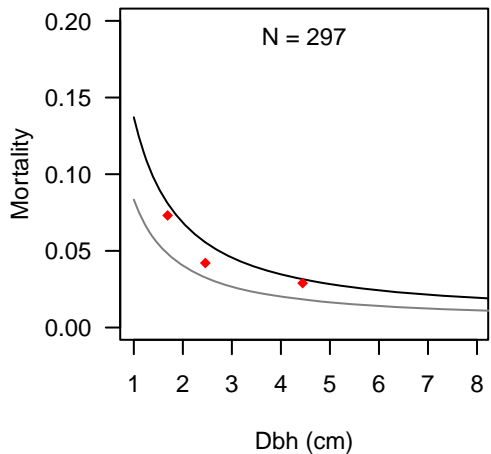


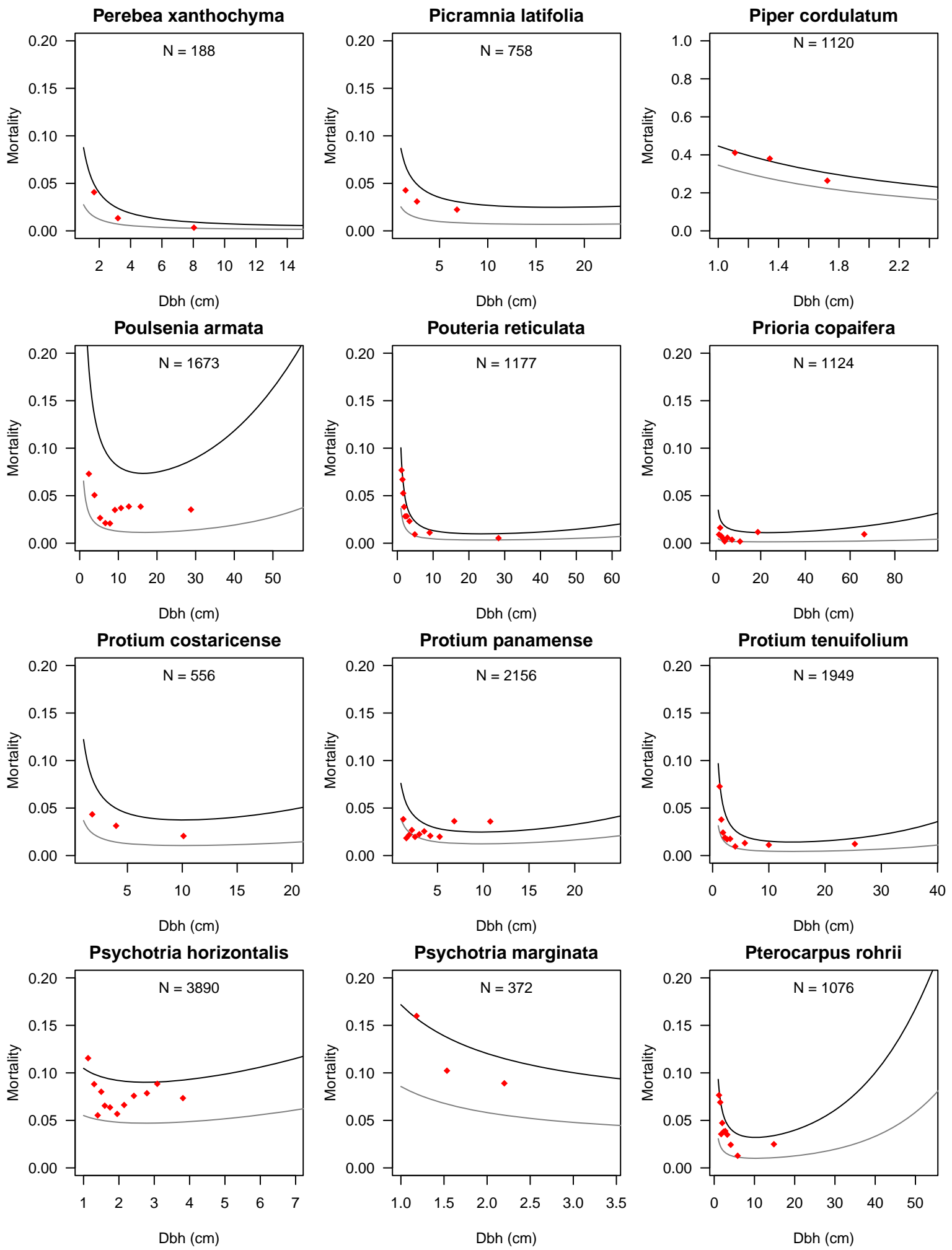


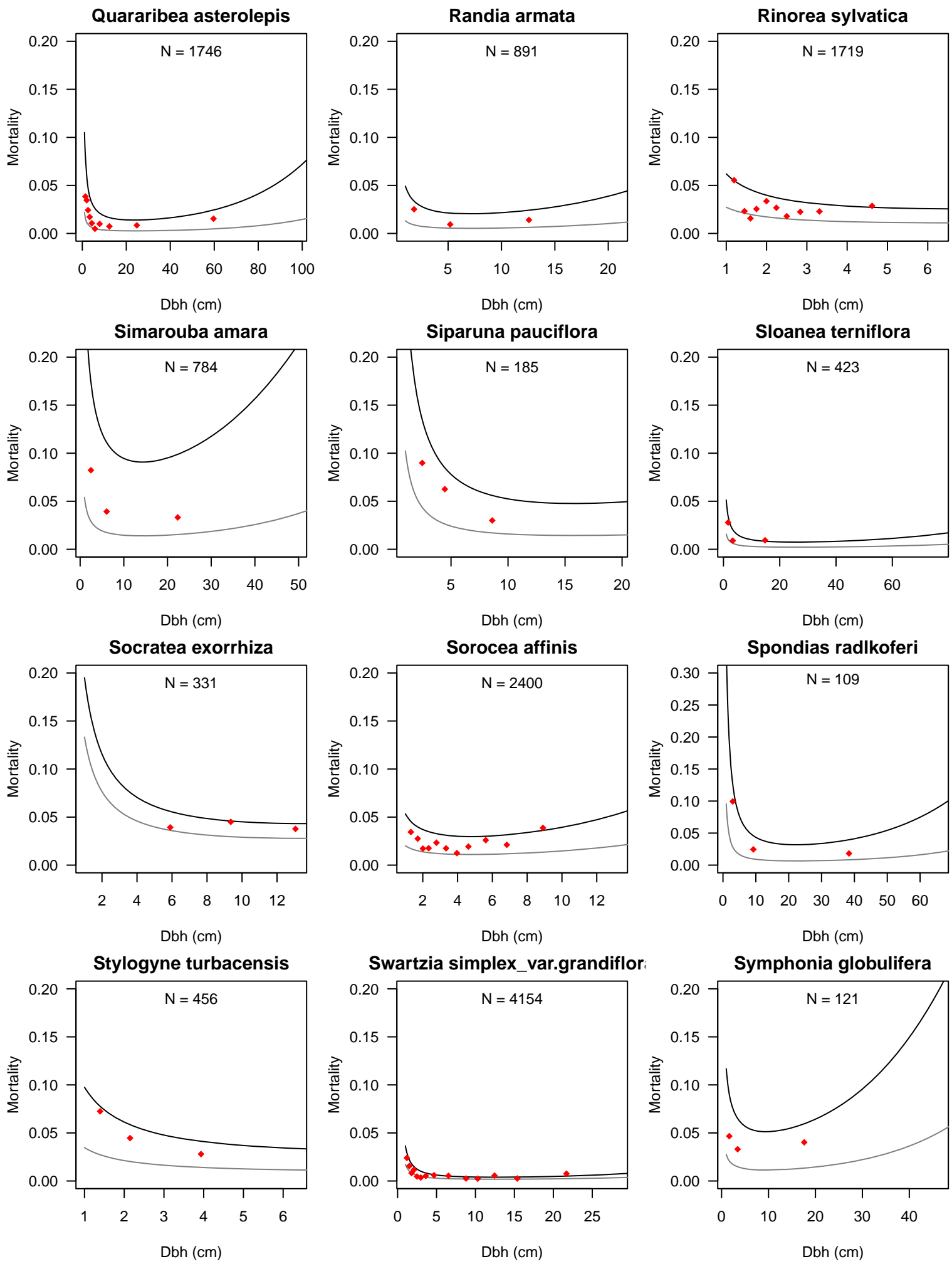


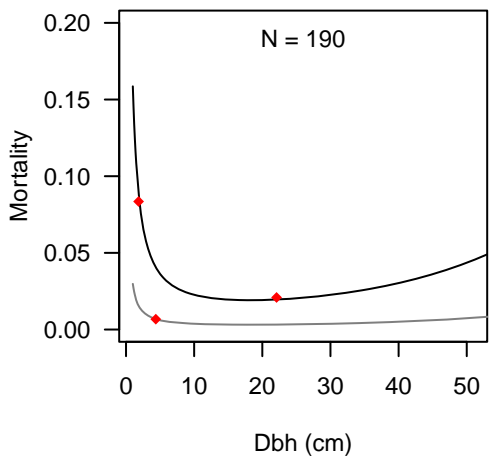
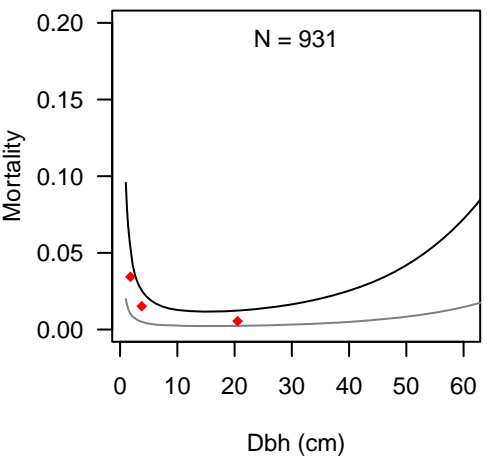
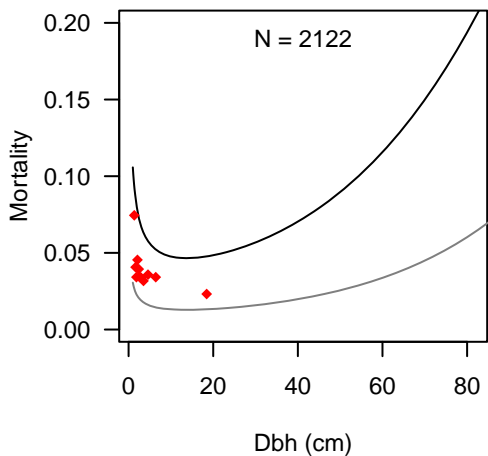
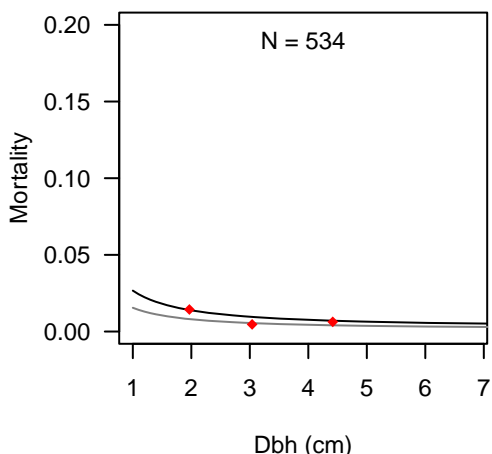
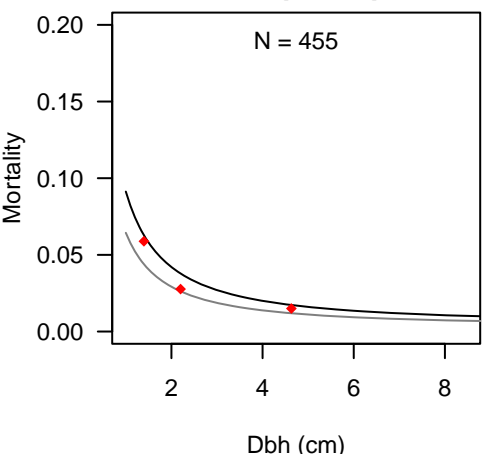
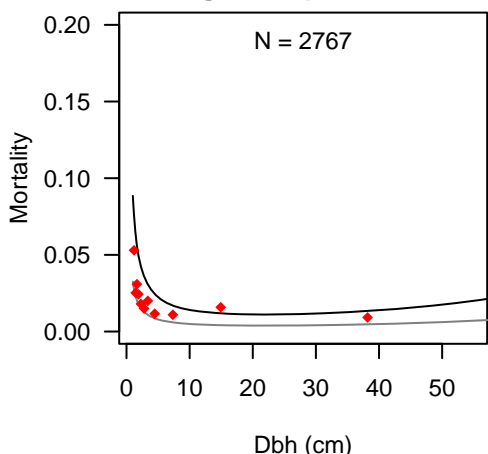
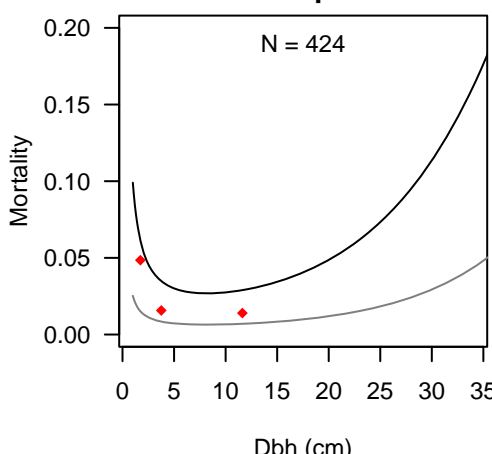
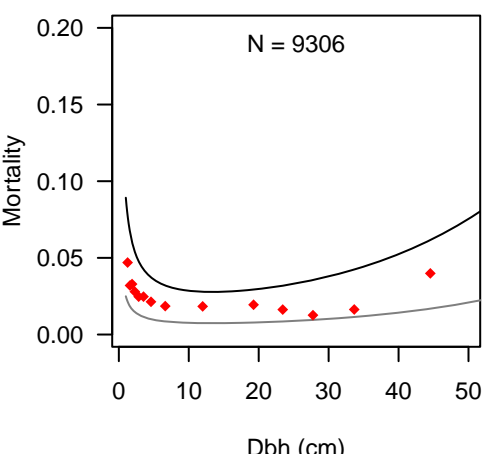
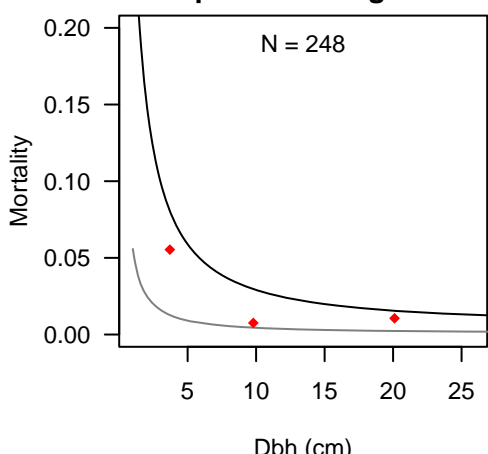
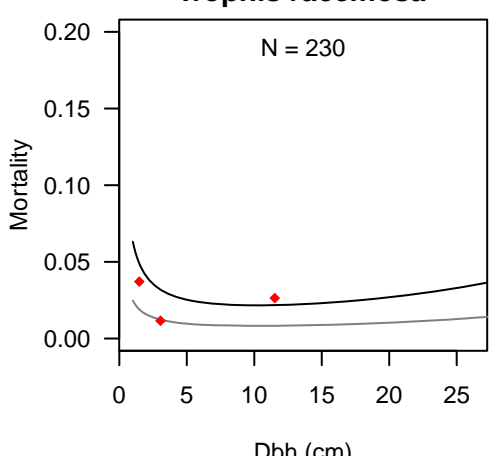
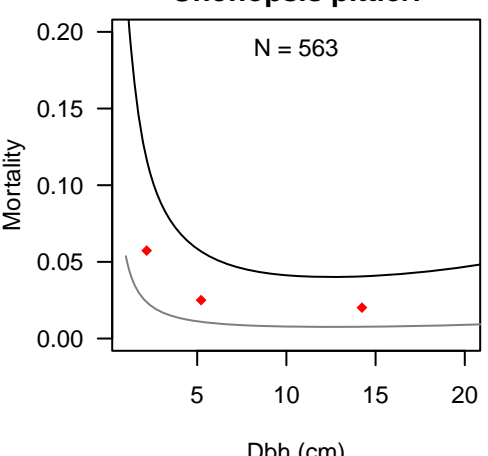




Miconia affinis**Miconia argentea****Mouriri myrtilloides****Nectandra cissiflora****Ocotea cernua****Ocotea puberula****Ocotea whitei****Oenocarpus mapora****Trophis caucana****Ouratea lucens****Palicourea guianensis****Pentagonia macrophylla**





Tabebuia rosea***Tabernaemontana arborea******Tachigali versicolor******Talisia nervosa******Talisia princeps******Tetragastris panamensis******Trichilia pallida******Trichilia tuberculata******Triplaris cumingiana******Trophis racemosa******Unonopsis pittieri******Virola sebifera***